

Spring 5-31-2010

Design of drug delivery strategies based on well-stirred experiments

Kumud Kanneganti
New Jersey Institute of Technology

Follow this and additional works at: <https://digitalcommons.njit.edu/theses>

 Part of the [Chemical Engineering Commons](#)

Recommended Citation

Kanneganti, Kumud, "Design of drug delivery strategies based on well-stirred experiments" (2010).
Theses. 57.
<https://digitalcommons.njit.edu/theses/57>

This Thesis is brought to you for free and open access by the Electronic Theses and Dissertations at Digital Commons @ NJIT. It has been accepted for inclusion in Theses by an authorized administrator of Digital Commons @ NJIT. For more information, please contact digitalcommons@njit.edu.

Copyright Warning & Restrictions

The copyright law of the United States (Title 17, United States Code) governs the making of photocopies or other reproductions of copyrighted material.

Under certain conditions specified in the law, libraries and archives are authorized to furnish a photocopy or other reproduction. One of these specified conditions is that the photocopy or reproduction is not to be “used for any purpose other than private study, scholarship, or research.” If a user makes a request for, or later uses, a photocopy or reproduction for purposes in excess of “fair use” that user may be liable for copyright infringement,

This institution reserves the right to refuse to accept a copying order if, in its judgment, fulfillment of the order would involve violation of copyright law.

Please Note: The author retains the copyright while the New Jersey Institute of Technology reserves the right to distribute this thesis or dissertation

Printing note: If you do not wish to print this page, then select “Pages from: first page # to: last page #” on the print dialog screen

The Van Houten library has removed some of the personal information and all signatures from the approval page and biographical sketches of theses and dissertations in order to protect the identity of NJIT graduates and faculty.

ABSTRACT

DESIGN OF DRUG DELIVERY STRATEGIES BASED ON WELL-STIRRED VESSEL EXPERIMENTS

by
Kumud Kanneganti

Drugs are generally administered to the human body via injections (IV) or through other paths such as the buccal, nasal routes. The main consideration when designing a medication schedule is to maintain a therapeutic level of the drug in the body during the course of treatment. To achieve this goal, when IV drug therapy is selected, particular importance has to be given to the dose to be injected and how to maintain the concentration of the pharmaceutical active ingredient (API) in the body between a Minimum Toxic Concentration (MTC) and a Minimum Effective Concentration (MEC). This therapeutic range varies with the drug and is designed so that the patient takes full benefit of the treatment while keeping potential risks or side effects to a minimum.

The aim of this thesis is to design drug administration protocols based on well-stirred vessel experiments that mimic one- and two-compartment pharmacokinetic models. A one-compartment model assumes that drug is evenly distributed in the body, which is represented by a beaker with an inlet and an outlet stream. In a two-compartment model, drug is distributed between the central and peripheral vessels. Only bolus and constant-rate infusion are considered in this study. Mathematical models are used to estimate the pharmacokinetic parameters and to derive administration strategies to be tested experimentally. Results show that the well-stirred vessel captures the behavior of one- and two-compartment models very well. The time-concentration profiles of a tracer in the compartments are functions of the kinetic parameters.

**DESIGN OF DRUG DELIVERY STRATEGIES BASED
ON WELL-STIRRED VESSEL EXPERIMENTS**

**by
Kumud Kanneganti**

**A Thesis
Submitted to the Faculty of
New Jersey Institute of Technology
in Partial Fulfillment of the Requirements for the Degree of
Master of Science in Chemical Engineering**

**Otto H. York Department of
Chemical, Biological and Pharmaceutical Engineering**

May 2010

Blank Page

APPROVAL PAGE

**DESIGN OF DRUG DELIVERY STRATEGIES BASED
ON WELL-STIRRED VESSEL EXPERIMENTS**

Kumud Kanneganti

Dr. Laurent Simon, Thesis Advisor	Date
Associate Professor, Otto H York Department of Chemical, Biological and Pharmaceutical Engineering, NJIT.	

Dr. Piero. M. Armenante, Committee Member	Date
Distinguished Professor, Otto H York Department of Chemical, Biological and Pharmaceutical Engineering, NJIT.	

Dr. Reginald. P. Tomkins, Committee Member	Date
Professor, Otto H York Department of Chemical, Biological and Pharmaceutical Engineering, NJIT.	

BIOGRAPHICAL SKETCH

Author: Kumud Kanneganti

Degree: Master of Science

Date: May 2010

Undergraduate and Graduate Education:

- Master of Science in Chemical Engineering,
New Jersey Institute of Technology, Newark, NJ, 2010
- Bachelor of Science in Chemical Engineering,
Nirma University, Ahmedabad, India, 2008

Major: Chemical Engineering

Publication:

Laurent Simon, Kumud Kanneganti and Kwang Seok Kim, *Drug transport and Pharmacokinetics for Chemical Engineering students*. Chemical Engineer Educator (To be published)

*To Mom and Dad, it is impossible to thank you for everything you've done,
from loving me unconditionally to raising me.
I am truly blessed to have the two of you in my life and could not have
asked for better role-models.*

And

*To God, for giving me strength when I needed it the most,
for giving me such wonderful and loving parents,
for giving me friends who stood by me through thick and thin,
and for giving me a good life.*

ACKNOWLEDGMENT

I would like to take this opportunity to express my gratitude towards Dr. Laurent Simon, Associate Professor, Otto H York Department of Chemical, Biological and Pharmaceutical Engineering for providing me with an opportunity to work with him. This not only gave me immense pleasure but also provided me with a platform to grow. I would like to thank him for his guidance and invaluable advice throughout the course of this study.

I am thankful to committee member, Dr. Piero M Armenante, Distinguished Professor, Otto H York Department of Chemical, Biological and Pharmaceutical Engineering for his timely advice and valuable inputs and a special thank you to Dr. Reginald P Tomkins, Associate Chair, Otto H York Department of Chemical, Biological and Pharmaceutical Engineering for his continuous encouragement throughout my stay at NJIT. I would also like to thank Mr. Kwang Seok Kim for his timely help and finally my family and friends for their unconditional love and support.

TABLE OF CONTENTS

Chapter	Page
1. INTRODUCTION.....	1
2. BACKGROUND.....	3
2.1 One-Compartment Model.....	3
2.1.1 IV Bolus.....	4
2.1.2 Multiple IV Boluses.....	5
2.1.3 Infusion.....	7
2.1.4 IV Boluses and Infusion.....	8
2.1.5 Experiments with One-Compartment model.....	8
2.2 Two-Compartment Model.....	11
2.2.1 IV Bolus.....	12
2.2.2 Multiple IV Boluses.....	15
2.2.3 Infusion.....	17
2.2.4 IV Boluses and Infusion.....	19
2.2.5 Experiments with Two-Compartment model.....	20
3. EXPERIMENTAL SECTION.....	23
3.1 Experiments on One-Compartment Model.....	23
3.1.1 Single IV Bolus.....	23
3.1.2 Multiple IV Boluses.....	24
3.1.3 Effect of Size of Dose and Dosage Interval.....	25
3.1.4 Effect of Time Dependent Kinetics.....	26

TABLE OF CONTENTS (Continued)

Chapter	Page
3.1.5 Infusion.....	26
3.1.6 IV boluses and Infusion.....	27
3.2 Experiments on Two-Compartment Model.....	28
3.2.1 Single IV Bolus.....	28
3.2.2 Multiple IV Boluses.....	28
3.2.3 Effect of Time Dependent Kinetics.....	29
3.2.4 Infusion.....	30
3.2.5 IV Boluses and Infusion.....	30
4. RESULTS AND DISCUSSIONS.....	32
4.1 Experiments on One-Compartment Model.....	32
4.1.1 Single IV Bolus.....	32
4.1.2 Multiple IV Boluses.....	34
4.1.3 Effect of Size of Dose and Dosage Interval.....	36
4.1.4 Effect of Time Dependent Kinetics.....	39
4.1.5 Infusion.....	42
4.1.6 IV Boluses and Infusion.....	43
4.2 Experiments on Two-Compartment Model.....	45
4.2.1 Single IV Bolus.....	45
4.2.2 Multiple IV Boluses.....	47
4.2.3 Effect of Time Dependent Kinetics.....	49

TABLE OF CONTENTS (Continued)

Chapter	Page
4.2.4 Infusion.....	53
4.2.5 IV Boluses and Infusion.....	54
5. CONCLUSION.....	55
5.1 Future Work.....	56
APPENDIX A MASS BALANCE EQUATIONS FOR EXPERIMENTAL SETUP OF TWO-COMPARTMENT MODEL.....	57
APPENDIX B LAPLACE TRANSFORM METHOD.....	60
APPENDIX C DATA ANALYSIS.....	63
C.1 Data Analysis on One-compartment Model.....	63
C.2 Data Analysis on Two-compartment Model.....	63
APPENDIX D MATHEMATICA CODE FOR OPTIMIZATION.....	66
D.1 Mathematica Code for the Optimization of Multiple IV Bolus Regimes.	66
D.2 Mathematica Code for the Optimization of IV Boluses with Infusion....	69
REFERENCES.....	80

LIST OF TABLES

Table	Page
2.1 Calibration Table for Concentration versus Absorbance.....	11

LIST OF FIGURES

Figure	Page
2.1 Representation of one-compartment model.	3
2.2 Representation of the experimental setup for one-compartment model.	4
2.3 Experimental setup of one-compartment model.	10
2.4 Representation of two-compartment model.	12
2.5 Representation of the experimental setup for two-compartment model.	13
2.6 Experimental setup of two-compartment model.	22
4.1 Plasma drug concentration-time profile for a single bolus dose. Loading dose is 0.04 g, $k_{el} = 0.028 \text{ second}^{-1}$. The symbols (♦) represent the experimental profile and (■) represent the calculated profile.	33
4.2 Plasma concentration profile due to one IV bolus (Nafcillin) : $C_p^0 = 29.1 \text{ } \mu\text{g/mL}$, $k_{el} = 0.483 \text{ hr}^{-1}$.	33
4.3 Plasma drug concentration time profile for a one compartment model with nine IV Boluses. Loading dose is 0.04 g, $k_{el} = 0.028 \text{ second}^{-1}$, $n = 9$ and $\tau = 60$ second. The symbols (♦) represent the experimental profile.	34
4.4 Theoretically calculated plasma drug concentration time profile for one compartment model with nine IV Boluses. Loading dose is 0.042 g, $k_{el} = 0.028 \text{ second}^{-1}$, $n = 9$ and $\tau = 60 \text{ sec}$. The symbols (■) represent the calculated profile.	35
4.5 Plasma concentration profile for a multiple IV bolus regimen. The parameters for nafcillin, $C_p^0 = 29.1 \text{ } \mu\text{g/mL}$ and $k_{el} = 0.483 \text{ hr}^{-1}$. For the simulation, $n = 10$ and $\tau = t_{1/2}$.	35
4.6 Plasma drug concentration time profile for one compartment model with nine IV Boluses with two drug sizes. Here, Dose # 1 is 0.073 g represented by (●) and Dose # 2 is 0.109 g represented by (■), $k_{el} = 0.028 \text{ second}^{-1}$ for both and $\tau = 45$ seconds.	37
4.7 Plasma drug concentration time profile for the change in dose interval. Dose # 1 = 0.073 g, $k_{el} = 0.028 \text{ second}^{-1}$ for $\tau = 45 \text{ sec}$ (●) and $\tau = 30 \text{ sec}$ (■).	38

LIST OF FIGURES (Continued)

Figure	Page
4.8 Plasma drug concentration time profile for the change in dose interval. Dose # 2 = 0.109 g, $k_{el} = 0.028 \text{ second}^{-1}$ for $\tau = 45 \text{ sec}$ (●) and $\tau = 30 \text{ sec}$ (■).	38
4.9 Change of the rate constant of elimination during the length of the experiment.	39
4.10 The comparison between the plasma drug concentration time profiles with a constant $k_{el} = 0.014 \text{ minute}^{-1}$ (●) and a plasma drug concentration time profile with varying k_{el} (■). Loading dose = 0.169 g and $\tau = 45 \text{ min}$.	40
4.11 The symbols (♦) represent the experimental concentration profile for $k_{el} = 0.014 \text{ min}^{-1}$ and $k_0 = 5.6 \text{ g/min}$.	42
4.12 Calculated concentration profile is represented by the symbols (■) for $k_{el} = 0.014 \text{ min}^{-1}$ and $k_0 = 5.6 \text{ g/min}$.	43
4.13 Plasma concentrations versus time for one IV bolus with infusion are represented by (■), with loading dose of 0.4 g, $k_{el} = 0.014 \text{ min}^{-1}$ and $k_0 = 5.6 \text{ g/min}$.	44
4.14 Plasma concentrations versus time for two (●) and four IV boluses (■) with loading dose as 0.4 g and $k_{el} = 0.014 \text{ min}^{-1}$ followed by a constant-rate infusion of $k_0 = 5.6 \text{ g/min}$.	44
4.15 Concentration profile for two-compartment model with initial dose 1.37 g. The symbols (▲) and (■) represent the profile for the central and peripheral compartment, respectively.	46
4.16 Calculated concentration profile for two compartment model, with a initial dose of 1.37 g. The symbols (♦) and (■) represent the profile for the central and peripheral compartment respectively.	46
4.17 Concentration profile for multiple boluses, with a loading dose of 0.82 g. The first and second maintenance doses are 0.314 g and 0.252 g, respectively. The kinetic rate constants are $k_{12} = 1.7999 \text{ hr}^{-1}$, $k_{21} = 2.9246 \text{ hr}^{-1}$ and $k_{el} = 0.2739 \text{ hr}^{-1}$. The symbols (♦) and (■) represent the profile for the central and peripheral compartment respectively.	48

LIST OF FIGURES (Continued)

Figure	Page
4.18 Calculated concentration profile for multiple boluses, with loading dose of 0.82 g. The first and second maintenance doses are 0.314 g and 0.252 g, respectively. The kinetic rate constants are $k_{12} = 1.7999 \text{ hr}^{-1}$, $k_{21} = 2.9246 \text{ hr}^{-1}$ and $k_{el} = 0.2739 \text{ hr}^{-1}$.	49
4.19 Concentration profile for one IV bolus of 1.37 g, where the symbols (♦) and (▲) represent the profile for the central and peripheral compartment respectively. The kinetic rate constants are $k_{12} = 1.7993 \text{ hr}^{-1}$, $k_{21} = 2.9246 \text{ hr}^{-1}$ and $k_{el} = 0.2739 \text{ hr}^{-1}$. Where as the symbols (■) and (X) represent the profile for central and peripheral compartment, respectively. The kinetic rate constants are $k_{12} = 1.4023 \text{ hr}^{-1}$, $k_{21} = 2.9954 \text{ hr}^{-1}$ and $k_{el} = 0.2815 \text{ hr}^{-1}$. The standard deviation for k_{12} , k_{21} and k_{el} are 0.291, 0.617 and 0.098, respectively.	50
4.20 Concentration profile for one IV bolus of 1.37 g, the symbols (♦) and (▲) represent the profile for the central and peripheral compartment respectively. The kinetic rate constants as $k_{12} = 1.7993 \text{ hr}^{-1}$, $k_{21} = 2.9246 \text{ hr}^{-1}$ and $k_{el} = 0.2739 \text{ hr}^{-1}$. Whereas the symbols (■) and (X) represent the profile for central and peripheral compartment respectively. The kinetic rate constants as $k_{12} = 1.6915 \text{ hr}^{-1}$, $k_{21} = 3.7948 \text{ hr}^{-1}$ and $k_{el} = 0.2794 \text{ hr}^{-1}$.	51
4.21 Concentration profile for one IV bolus of 1.37 g, the symbols (♦) and (▲) represent the profile for the central and peripheral compartment respectively. The kinetic rate constants as $k_{12} = 1.7993 \text{ hr}^{-1}$, $k_{21} = 2.9246 \text{ hr}^{-1}$ and $k_{el} = 0.2739 \text{ hr}^{-1}$. Whereas the symbols (■) and (X) represent the profile for central and peripheral compartment respectively. The kinetic rate constants as $k_{12} = 1.6566 \text{ hr}^{-1}$, $k_{21} = 3.0903 \text{ hr}^{-1}$ and $k_{el} = 0.4129 \text{ hr}^{-1}$.	52
4.22 Concentration profile for IV infusion of 0.695 g of drug having an infusion rate $R = 0.996 \text{ g/hr}$. The kinetic rate constants are $k_{12} = 1.0968 \text{ hr}^{-1}$, $k_{21} = 2.3596 \text{ hr}^{-1}$ and $k_{el} = 1.4335 \text{ hr}^{-1}$. Here, the symbols (♦) represent the experimental profile and (■) represents the calculated profile.	53
4.23 Concentration profile for three IV boluses with infusion of 0.695 g of drug with a loading dose of 0.82 g. The first and second maintenance doses are 0.201 g and 0.196 g respectively. The infusion rate was $R = 0.996 \text{ g/hr}$. The kinetic rate constants are $k_{12} = 1.0968 \text{ hr}^{-1}$, $k_{21} = 2.3596 \text{ hr}^{-1}$ and $k_{el} = 1.4335 \text{ hr}^{-1}$. The symbols (♦) and (■) represent the profile for the central and peripheral compartment, respectively.	54

CHAPTER 1

INTRODUCTION

Drugs are generally administered to the human body via injections (IV) or through other paths such as the buccal and nasal routes. An injection (IV) used to administer the active pharmaceutical ingredient (API) [1], introduces the API directly into the blood and hence into the circulatory system, which distributes the drug throughout the body in a very short time. This route also avoids the absorption process. When an API is administered, absorption, distribution, metabolism and excretion, contribute towards the continuously changing concentration of the drug in the body. Several tests can be carried out to study the effects of these individual processes on the drug concentration. However, only excretion is simulated in this study.

The objective of a drug therapy is to achieve and maintain an effective drug concentration in the body. This is also the main consideration when designing a medication schedule during the course of treatment. To achieve this goal, when IV drug therapy is selected, particular importance has to be given to the dose to be injected and how to maintain the concentration of the API in the body between a Minimum Toxic Concentration (MTC) and a Minimum Effective Concentration (MEC). This therapeutic range varies with the drug and is designed so that the patient takes full benefit of the treatment, while keeping potential risks or side effects to a minimum.

The drug absorption begins as soon as the drug is administered into the body. As a result the medicament does not remain in a single location, but is distributed throughout the body until it is totally removed. The various body locations to which a drug travels

may be viewed as separate compartments, each containing some fraction of the administered dose of the drug [2]. Each compartment is a specific organ or a site. Hence the body is said to be a sum of all the compartments [3]. In this study, the body is assumed to consist of one or two compartments.

The aim of this thesis is to design drug administration protocols based on well-stirred vessel experiments that mimic one- and two-compartment pharmacokinetic models. A one-compartment model assumes that the body is a single compartment and that the drug is evenly distributed in the body, which is represented by a beaker with an inlet and an outlet stream. A two-compartment model, on the other hand assumes that the body is made of two compartments, namely, the blood and the tissue [2]. The drug is distributed between the two chambers. In this description, the blood and tissue are represented by the central and peripheral compartments, respectively. Time concentration profiles are different in the two compartments. Only bolus and constant-rate infusion are considered in this study. Mathematical models are used to estimate the pharmacokinetic parameters and to derive administration strategies that are tested experimentally.

CHAPTER 2

BACKGROUND

2.1 One-compartment Model

The one-compartment model is the simplest system that can be used to describe drug distribution and elimination in the body. One-compartment model assumes that the pharmaceutical enters and leaves the body, which acts like a single uniform chamber represented in Figure 2.1.

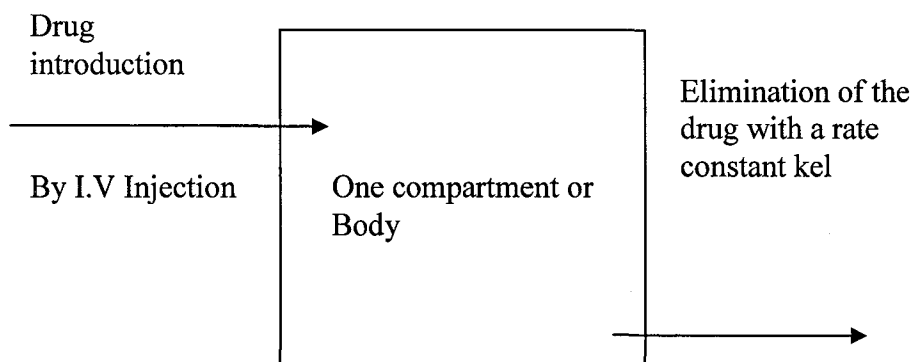


Figure 2.1 Representation of one-compartment model.

In this framework, no distinction is drawn between the drug concentration in the blood and the surrounding tissue. Hence, as soon as the active pharmaceutical ingredient enters the body, it is instantaneously distributed throughout the volume.

Figure 2.2 shows the diagrammatic representation of the experimental setup used to mimic the pharmacokinetics of a drug in one-compartment model. The equations governing the process are derived using Figure 2.2 as a basis.

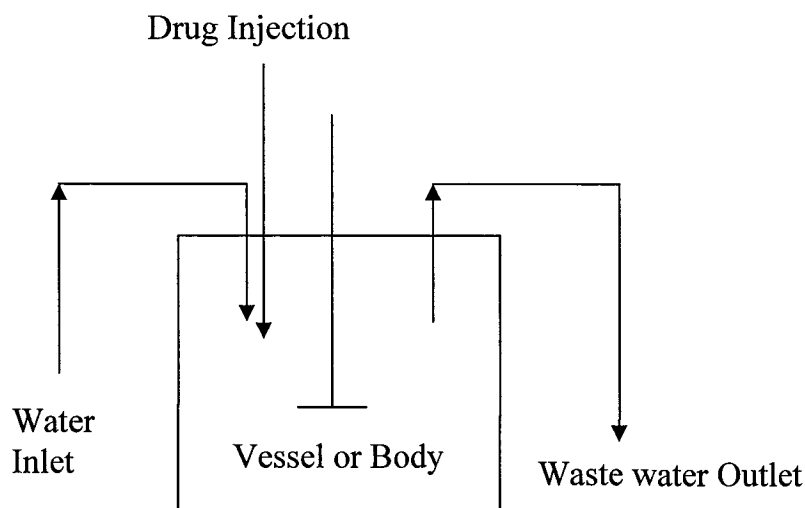


Figure 2.2 Representation of the experimental setup for one-compartment model.

2.1.1 IV Bolus

An intravenous injection (IV bolus) ensures that a certain amount of drug is made available in the system instantaneously. The kinetic model is derived by first noting that the situation is similar to the addition of a rapid bolus dose to a Continuously Stirred Tank Reactor (CSTR) or vessel (Figure 2.2). An outlet stream represents the drug elimination.

The mass balance over the constant-volume system in Figure 2.2 gives a differential equation:

$$\frac{dC_p}{dt} = -k_{el}C_p \quad (2.1)$$

Where k_{el} is a first-order elimination rate constant (min^{-1}), C_p is the concentration of the drug in the plasma (g/L or g/mL) at corresponding time t (sec/min). The integration of equation (1) gives:

$$C_p = C_p^0 e^{-k_{el} \times t} \quad (2.2)$$

The elimination rate constant is calculated by plotting the concentration against the time, C_p^0 is the drug concentration introduced in the distribution volume V (ml or L). The amount drug in the system can be calculated if the elimination rate constant, the volume of distribution and the amount of drug administered at $t = 0$ are known, for one IV bolus.

2.1.2 Multiple IV Boluses

After a single dose, the plasma drug concentration immediately rises and declines as it is being eliminated from the body via a first-order process. For an effective treatment, C_p should be maintained between a minimum effective concentration (MEC) and a minimum toxic concentration (MTC) for the duration of therapy. Because such a profile is not possible with one intake, multiple-dosing regime is often prescribed. Subsequent doses taken at appropriate time intervals lead to the accumulation of medicament in the body and therefore, help to keep a desired range.

The concentration at the end of the first dosing interval is obtained from Equation 2.2:

$$C_{p1}^{\tau} = C_{p1}^0 e^{-k_{el} \times \tau} \quad (2.3)$$

where the τ refers to the time since the last dose and the subscript “1” is the number of doses (i.e. in this case, one dose).

This gives the plasma concentrations at the end of first interval, where t is the dosing interval in seconds or minutes or hours.

At the beginning of the second interval, the concentration becomes,

$$C_{p2}^0 = C_{p1}^\tau + C_{p1}^0 \quad (2.4)$$

$$C_{p2}^0 = C_{p1}^t + C_{p1}^0 = C_{p1}^0 * e^{-K_{el} * t} + C_{p1}^0 \quad (2.5)$$

At the end of the second dose interval, the concentration becomes

$$C_{p2}^t = [C_{p1}^0 * e^{-K_{el} * t} + C_{p1}^0] * e^{-K_{el} * t} \quad (2.6)$$

This calculation results in a geometric series with each term $e^{-K_{el} * t}$ times the preceding term. Hence, for n doses, the concentration introduced will be

$$C_{pn}^0 = C_{p1}^0 + C_{p1}^0 * e^{-K_{el} * t} + C_{p1}^0 * (e^{-K_{el} * t})^2 + \dots + C_{p1}^0 * (e^{-K_{el} * t})^{n-1} \quad (2.7)$$

And the concentration at any time t after n doses i.e., C_p Immediately after the nth dose is given by

$$C_{pn}^t = C_{p1}^0 * e^{-K_{el} * t} + C_{p1}^0 * (e^{-K_{el} * t})^2 + C_{p1}^0 * (e^{-K_{el} * t})^3 + \dots + C_{p1}^0 * (e^{-K_{el} * t})^n \quad (2.8)$$

After further manipulations, the equations can be written as:

$$C_{pn}^0 = C_{p1}^0 * \left[\frac{1 - (e^{-K_{el} * \tau})^n}{1 - e^{-K_{el} * \tau}} \right] = C_{p1}^0 * \left[\frac{1 - e^{-n * K_{el} * \tau}}{1 - e^{-K_{el} * \tau}} \right] \quad (2.9)$$

and

$$C_{pn}^t = C_{p1}^0 * \left[\frac{1 - (e^{-K_{el} * \tau})^n}{1 - e^{-K_{el} * \tau}} \right] * e^{-K_{el} * t} = C_{p1}^0 * \left[\frac{1 - e^{-n * K_{el} * \tau}}{1 - e^{-K_{el} * \tau}} \right] * e^{-K_{el} * t} \quad (2.10)$$

respectively.

Equations are derived for maximum (C_{pmax}) and minimum (C_{pmin}) concentrations that can be achieved after an infinite number of boluses:

$$C_{p\infty}^0 = C_{pmax} = C_{p1}^0 * \left[\frac{1}{1 - e^{-kel*t}} \right] \quad (2.11)$$

and

$$C_{p\infty}^t = C_{pmin} = C_{p1}^0 * \left[\frac{e^{-kel*t}}{1 - e^{-kel*t}} \right] \quad (2.12)$$

2.1.3 Infusion

Drugs are administered intravenously in the form of a bolus dose or infused relatively slowly through a vein into the plasma at a constant or zero-order rate. One of the main advantages of an IV infusion is that an effective constant plasma drug concentration can be achieved, thereby eliminating the fluctuations observed in bolus IV dosing.

An infusion rate term is added to the mass balance of one-compartment model, to give:

$$\frac{dC_p}{dt} = \frac{k_0}{V} - k_{el} * C_p \quad (2.13)$$

In this formulation, k_0 is the input and $V * k_{el} * C_p$ is the output.

The integration of Equation (2.13) gives:

$$C_p = \frac{k_0}{V * k_{el}} (1 - e^{-k_{el}*t}) \quad (2.14)$$

where,

k_0 = infusion rate (Zero order) (g/hr)

kel = elimination rate constant (First order) (min^{-1})

C_p = concentration in Plasma (g/L)

V = distribution volume (mL) 200 mL

t = time (minute)

2.1.4 IV Boluses and Infusion

An initial bolus is given prior to infusion to reach the desired concentration as quickly as possible. The concentration of the drug in body after an IV bolus is described as:

$$\frac{dC_p}{dt} = \frac{k_0}{V} - k_{el} * C_p \quad (2.15)$$

with initial condition of $C_p(0) = C_0$.

The integration of Equation (2.15) gives:

$$C_p = C_0 * e^{-k_{el} * t} + \frac{k_0}{V * k_{el}} (1 - e^{-k_{el} * t}) \quad (2.16)$$

2.1.5 Experiments with one-compartment Model

There were various experiments performed using one-compartment model. The experiments were performed for single and multiple IV boluses, infusion with and without IV boluses. The effect of the model parameters on C_p was also studied. The materials and the experimental setup are given below:

Materials and Experimental Setup

• Variable flow-rate pump	2	(Clearance and water supply pump)
• 250-mL or 200-mL Beaker	1	(Central compartment)
• 4-L Beaker	2	(Water reservoir and waste beaker)
• Stopwatch	1	(Time measurement)
• 10-mL Graduate cylinder	1	(Flow rate calibration)
• Pipette	1	(Bolus drug administration)
• Rubber tubes		(Fluid transport)
• Magnetic stirrer	1	(Liquid mixing in central compartment)
• Magnetic bar	1	(Liquid mixing in central compartment)
• Potassium permanganate		(Drug)
• Spectrophotometer		(Absorbance/concentration measurement)
• Cuvette	4	(Sample in spectrophotometer)
• Laboratory stand	1	(Rubber tubes mounting)
• Clamp	4	(Rubber tubes mounting)
• Transfer pipette	1	(Drug administration)

The apparatus is shown in the Figure 2.3. The beaker with the KMnO_4 solution was placed on a magnetic stirrer. A pump was used to mimic drug clearance from the body (i.e., waste pump). Water was introduced with the same rate as the pump used to mimic drug clearance, in order to maintain a constant volume of liquid in the central compartment. The rubber tubes are fastened firmly with clamps.

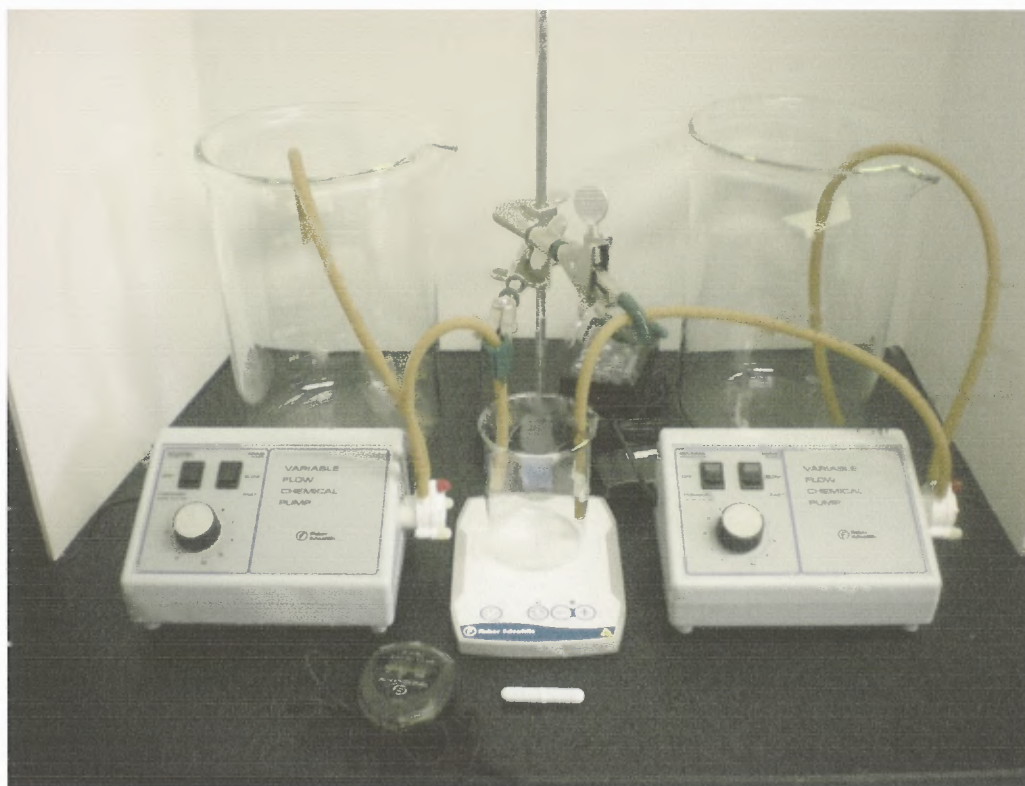


Figure 2.3 Experimental setup of one-compartment model.

Method of Measuring Concentration

A spectrophotometer is used to measure the concentration of KMnO_4 in the solution. A calibration curve was developed to relate the concentration with the absorbance reading at a wavelength of 530 nm. The solution prepared for this purpose is 2 g KMnO_4 in 1000ml water (i.e., concentration is 0.002 g/ml). The data are shown in Table 2.1.

Table 2.1 Calibration Table for Concentration versus Absorbance

Absorbance (A)	Concentration (g/ml)
0.126	0.002
0.063	0.001
0.032	0.0005
0.016	0.00025

The relationship that results from the above table is $C = 0.016 \cdot A$, where C is concentration in g/ml and A is the absorbance. Hence, the relationship between the concentration of the drug and the absorbance is established. This relationship is used to then record the concentration of the drug during the experiments with one-compartment model.

2.2 Two-compartment Model

A two-compartment model is used to represent the drug absorption, distribution and elimination in the body. This representation addresses cases in which the concentration profiles are different in the blood and surrounding tissue.

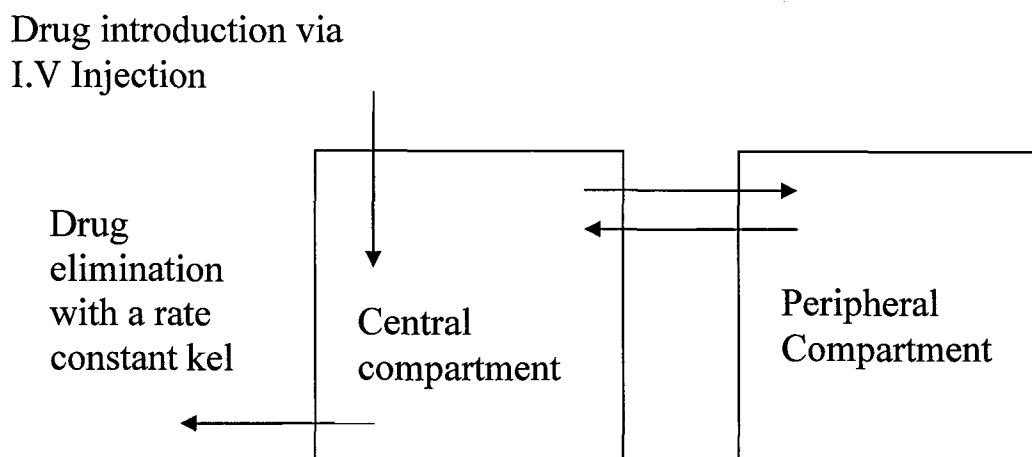


Figure 2.4 Representation of two-compartment model.

2.2.1 IV Bolus

In a two-compartment framework, one vessel, representing the blood and the extracellular fluid is the central compartment. The highly perfused tissues are represented by the other vessel, which is the peripheral compartment. The drug distributes rapidly and uniformly in the central compartment whereas the distribution is slower in the peripheral compartment.

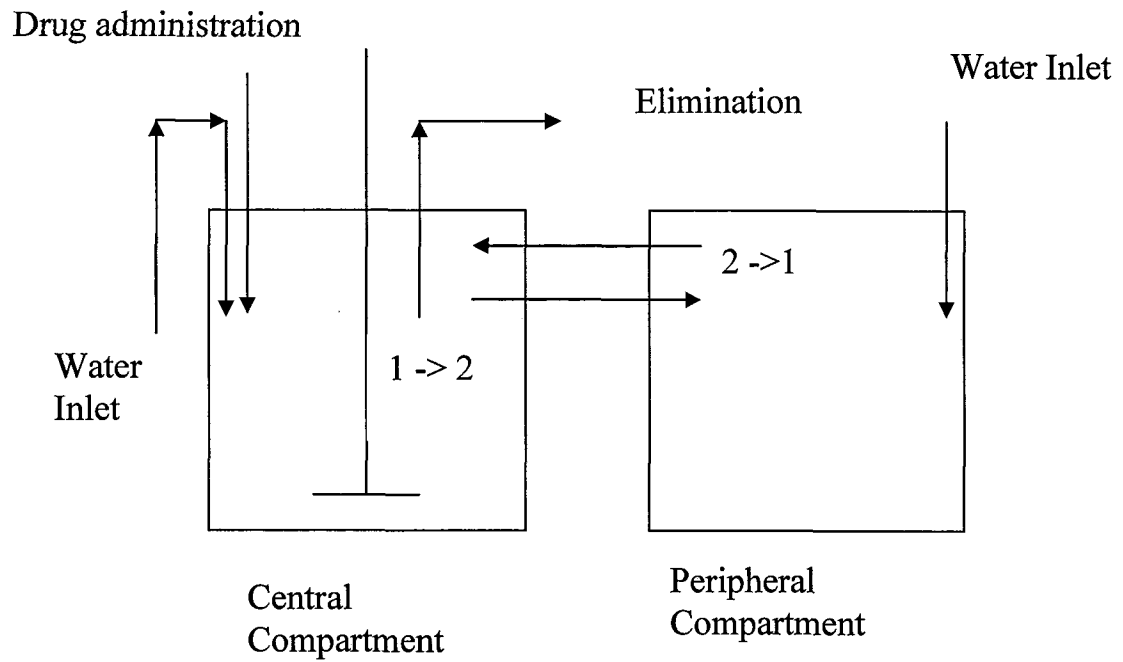


Figure 2.5 Representation of the experimental setup for two-compartment model.

Mass balances over the system in Figure 2.5 give,

$$\frac{dC_1}{dt} = -(k_{12} + k_{el})C_1 + k_{21}C_2 \quad (2.17)$$

and

$$\frac{dC_2}{dt} = -k_{21}C_2 + k_{12}C_1 \quad (2.18)$$

The mass balance equations are derived and shown in the Appendix A,

with the initial conditions:

$$C_1(0) = C_{10}$$

and

$$C_2(0) = 0$$

Applying the Laplace transform as discussed in Appendix B,

$$L\{f(t)\} = \bar{f}(s)$$

to Equations.(2.17) and (2.18), we obtain

$$s\bar{C}_1 - C_{10} = -(k_{12} + k_{el})\bar{C}_1 + k_{21}\bar{C}_2 \quad (2.19)$$

and

$$s\bar{C}_2 = k_{12}\bar{C}_1 - k_{21}\bar{C}_2 \quad (2.20)$$

From the above equation we have,

$$\bar{C}_2 = \frac{k_{12}}{(s + k_{21})} \bar{C}_1 \quad (2.21)$$

Substitution of Equation (2.21) into Equation (2.19) yields

$$\bar{C}_1 = \frac{(s + k_{21})C_{10}}{(s^2 + (k_{12} + k_{21} + k_{el})s + k_{el}k_{21})} \quad (2.22)$$

and

$$\bar{C}_2 = \frac{k_{12}C_{10}}{(s^2 + (k_{12} + k_{21} + k_{el})s + k_{el}k_{21})} \quad (2.23)$$

Equation (2.22) can be rearranged to give

$$\bar{C}_1 = \frac{(s + k_{21})C_{10}}{(s + a)(s + b)} \quad (2.24)$$

Equation (2.24) can be written as

$$\bar{C}_1 = \frac{A^*C_{10}}{(s+a)} + \frac{B^*C_{10}}{(s+b)} = \frac{(a - k_{21})C_{10}}{(a - b)(s + a)} - \frac{(b - k_{21})C_{10}}{(a - b)(s + b)} \quad (2.25)$$

and

$$\bar{C}_2 = \frac{D^*C_{10}}{(s+a)} + \frac{E^*C_{10}}{(s+b)} = -\frac{k_{12}C_{10}}{(a-b)(s+a)} + \frac{k_{12}C_{10}}{(a-b)(s+b)} \quad (2.26)$$

where a and b are both given by:

$$a = \frac{-(k_{12} + k_{21} + k_{el}) + \sqrt{(k_{12} + k_{21} + k_{el})^2 - 4k_{el}k_{21}}}{2}$$

$$b = \frac{-(k_{12} + k_{21} + k_{el}) - \sqrt{(k_{12} + k_{21} + k_{el})^2 - 4k_{el}k_{21}}}{2}$$

Here, both a and b are distinct and real because

$$\begin{aligned} (k_{12} + k_{21} + k_{el})^2 - 4k_{el}k_{21} &= k_{12}^2 + k_{21}^2 + k_{el}^2 + 2k_{12}k_{21} + 2k_{21}k_{el} + 2k_{12}k_{el} - 4k_{el}k_{21} \\ &= k_{12}^2 + k_{21}^2 + k_{el}^2 + 2k_{12}k_{21} - 2k_{21}k_{el} + 2k_{12}k_{el} \\ &= k_{12}^2 + (k_{21} - k_{el})^2 + 2k_{12}(k_{21} + k_{el}) > 0 \end{aligned}$$

The inverse Laplace transform of Equations (2.25) and (2.26) are

$$C_1 = \frac{(a - k_{21})C_{10}}{(a - b)}e^{-a^*t} - \frac{(b - k_{21})C_{10}}{(a - b)}e^{-b^*t} \quad (2.27)$$

and

$$C_2 = -\frac{k_{12}C_{10}}{(a - b)}e^{-a^*t} + \frac{k_{12}C_{10}}{(a - b)}e^{-b^*t} \quad (2.28)$$

2.2.2 Multiple IV Boluses

Multiple-dosing regime is often prescribed to maintain the plasma drug concentration between a minimum effective concentration (MEC) and a minimum toxic concentration (MTC) for the duration of the therapy. Equations (2.17) and (2.18) give the mass balance over the system defined in Figure 2.5. The initial conditions for this case are:

$$C_1(0) = C_{10}$$

and

$$C_2(0) = C_{20}$$

Applying the Laplace transform to Equations (2.17) and (2.18) we obtain

$$\bar{C}_1 = \frac{(s + k_{21})C_{10} + C_{20}k_{21}}{(s^2 + (k_{12} + k_{21} + k_{el})s + k_{el}k_{21})} \quad (2.29)$$

and

$$\bar{C}_2 = \frac{k_{12}C_{10} + C_{20}(k_{12} + k_{el} + s)k_{21}}{k_{12}k_{21} - (s + k_{21})(k_{12} + k_{el} + s)} \quad (2.30)$$

Equation (2.29) can be written as

$$\begin{aligned} \bar{C}_1 &= \frac{A^*C_{10}}{(s+a)} + \frac{B^*C_{10}}{(s+b)} + \frac{C^*C_{20}}{(s+a)} + \frac{D^*C_{20}}{(s+b)} \\ &= \frac{(a - k_{21})C_{10}}{(a-b)(s+a)} - \frac{(b - k_{21})C_{10}}{(a-b)(s+b)} - \frac{C_{20}k_{21}}{(a-b)(s+a)} + \frac{C_{20}k_{21}}{(a-b)(s+b)} \end{aligned} \quad (2.31)$$

The inverse Laplace transform of Equations (2.31) and (2.30) give

$$C_1 = \frac{(a - k_{21})C_{10}e^{-a^*t}}{(a-b)} - \frac{(b - k_{21})C_{10}e^{-b^*t}}{(a-b)} - \frac{C_{20}k_{21}e^{-a^*t}}{(a-b)} + \frac{C_{20}k_{21}e^{-b^*t}}{(a-b)} \quad (2.33)$$

and

$$C_2 = \frac{1}{2d} \left(-2C_{10}k_{12}e^{-a^*t} + 2C_{10}k_{12}e^{-b^*t} + C_{20}(-k_{12} + k_{21} - k_{el} + d)e^{-a^*t} + C_{20}(k_{12} - k_{21} + k_{el} + d)e^{-b^*t} \right) \quad (2.34)$$

$$\text{where, } d = \sqrt{(k_{12} + k_{21} + k_{el})^2 - 4k_{21}k_{el}}$$

Here, both a and b are distinct and real as discussed in the case of IV Bolus.

2.2.3 Infusion

Many drugs are administered by IV infusion. This requires the drug, to distribute itself in the tissue and reach equilibrium with the plasma drug concentration.

Equations (2.17) and (2.18) represent component balance over the system defined in Figure 2.5. An input term is added, in this case. Let R be that infusion rate term in (g/hr).

$$\frac{dC_1}{dt} = \frac{R}{V_1} - (k_{12} + k_{el})C_1 + k_{21}C_2 \quad (2.35)$$

and

$$\frac{dC_2}{dt} = -k_{21}C_2 + k_{12}C_1 \quad (2.36)$$

with the same initial conditions as in multiple IV boluses.

Applying the Laplace transform to Equations (2.35) and (2.36) we obtain,

$$s\bar{C}_1 = \frac{R}{V_1s} - (k_{12} + k_{el})\bar{C}_1 + k_{21}\bar{C}_2 \quad (2.37)$$

and

$$s\bar{C}_2 = k_{12}\bar{C}_1 - k_{21}\bar{C}_2 \quad (2.38)$$

From the above Equation (2.38) we have,

$$\bar{C}_2 = \frac{k_{12}}{(s + k_{21})} \bar{C}_1 \quad (2.39)$$

Substitution of Equation (2.39) into (2.37) yields

$$\bar{C}_1 = \frac{R'(s + k_{21})}{s(s^2 + (k_{12} + k_{21} + k_{el})s + k_{el}k_{21})} \quad (2.40)$$

and

$$\bar{C}_2 = \frac{R'k_{12}}{s(s^2 + (k_{12} + k_{21} + k_{el})s + k_{el}k_{21})} \quad (2.41)$$

Here, $R' = \frac{R}{V_1}$ and also the above equation can be written as

$$\begin{aligned} \bar{C}_1 &= \frac{A^*R'}{(s)} + \frac{B^*R'}{(s+a)} + \frac{C^*R'}{(s+b)} \\ &= \frac{k_{21}R'}{(a*b)(s)} + \frac{(k_{21} - a)^*R'}{a(a-b)(s+a)} - \frac{(b - k_{21})^*R'}{b(a-b)(s+b)} \end{aligned} \quad (2.42)$$

and

$$\begin{aligned} \bar{C}_2 &= \frac{A^*R'}{(s)} + \frac{B^*R'}{(s+a)} + \frac{C^*R'}{(s+b)} \\ &= \frac{k_{12}R'}{(a*b)(s)} + \frac{k_{12}^*R'}{a(a-b)(s+a)} - \frac{k_{12}^*R'}{b(a-b)(s+b)} \end{aligned} \quad (2.43)$$

The inverse Laplace of the above equations gives

$$C_1 = \frac{k_{21} * R'}{(a * b)} + \frac{(k_{21} - a) * R' * e^{-a * t}}{a(a - b)} - \frac{(b - k_{21}) * R' * e^{-b * t}}{b(a - b)} \quad (2.44)$$

$$C_2 = \frac{k_{12} * R'}{(a * b)} + \frac{k_{12} * R' * e^{-a * t}}{a(a - b)} - \frac{k_{12} * R' * e^{-b * t}}{b(a - b)} \quad (2.45)$$

Here, both a and b are distinct and real as discussed in the case of IV Bolus.

2.2.4 IV Boluses and Infusion

It is always desirable to achieve a rapid therapeutic drug level in plasma by using a loading dose. The drug distributes slowly into extravascular tissues and hence the drug equilibrium is not immediate.

The mass balance is the same as in the infusion case but the initial conditions are,

$$C_1(0) = C_{10}$$

and

$$C_2(0) = C_{20}$$

Applying the Laplace transform to Equations (2.35) and (2.36), we obtain

$$s\bar{C}_1 - C_{10} = \frac{R'}{s} - (k_{12} + k_{el})\bar{C}_1 + k_{21}\bar{C}_2 \quad (2.46)$$

and

$$s\bar{C}_2 - C_{20} = k_{12}\bar{C}_1 - k_{21}\bar{C}_2 \quad (2.47)$$

From the above Equation (2.47) we have:

$$\bar{C}_2 = \frac{k_{12}\bar{C}_1 + C_{20}}{(s + k_{21})} \quad (2.48)$$

Substitution of Equation (2.48) into (2.47) yields

$$\bar{C}_1 = \frac{C_{10}s^2 + s(C_{10}k_{21} + C_{20}k_{21} + R') + k_{21}R'}{s(s+a)(s+b)} \quad (2.49)$$

The above equation can now be written as

$$\begin{aligned} \bar{C}_1 &= \frac{A}{s} + \frac{B}{s+a} + \frac{C}{s+b} \\ &= \frac{k_{21}R'}{(a*b)s} + \frac{bC_{10}k_{21} + bC_{20}k_{21} + R'b - k_{21}R' - C_{10}b^2}{(s+b)b(a-b)} + \frac{C_{10}a^2 - ak_{21}(C_{10} + C_{20}) - R'a - k_{21}R'}{(s+a)a(a-b)} \end{aligned} \quad (2.50)$$

The inverse Laplace of the above equation gives

$$\begin{aligned} C_1 &= \frac{k_{21}R'}{(a*b)} + \frac{(bC_{10}k_{21} + bC_{20}k_{21} + R'b - k_{21}R' - C_{10}b^2)e^{-b*t}}{b(a-b)} \\ &\quad + \frac{(C_{10}a^2 - ak_{21}(C_{10} + C_{20}) - Ra - k_{21}R')e^{-a*t}}{a(a-b)} \end{aligned} \quad (2.51)$$

2.2.6 Experiments with two-compartment Model

There were various experiments performed using one-compartment model. The experiments were performed for single and multiple IV Boluses, infusion with and without IV boluses. The effect of the model parameter on C_p was also studied. The materials and the experimental setup are given below:

Materials and Experimental Setup

- | | | |
|---------------------------|---|--------------------------------------|
| • Variable flow-rate pump | 5 | (Clearance and water supply pump) |
| • 250-mL or 200-mL Beaker | 2 | (Central and Peripheral compartment) |
| • 4-L Beaker | 2 | (Water reservoir and waste beaker) |
| • Stopwatch | 1 | (Time measurement) |
| • 10-mL Graduate cylinder | 1 | (Flow rate calibration) |
| • Pipette | 2 | (Bolus drug administration) |

• Rubber tubes		(Fluid transport)
• Magnetic stirrer	2	(Liquid mixing in central compartment)
• Magnetic bar	2	(Liquid mixing in central compartment)
• Potassium permanganate		(Drug)
• Spectrophotometer		(Absorbance/concentration measurement)
• Cuvette	8	(Sample in spectrophotometer)
• Laboratory stand	2	(Rubber tubes mounting)
• Clamp	4	(Rubber tubes mounting)
• Transfer pipette	1	(Drug administration)

The apparatus is shown in the Figure 2.6. The beakers with the water were placed on a magnetic stirrer. A pump was used to mimic drug clearance from the body (i.e., waste pump). Water was introduced with different rates into both the vessels, in order to maintain a constant volume of liquid in the central compartment. Two more pumps were used to transfer fluid from the central to the peripheral compartment and vice versa. The rubber tubes are fastened firmly with clamps.



Figure 2.6 Experimental setup of two-compartment model.

Method of Measuring Concentration

The procedure is similar to the one used in the case of one-compartment model. The same calibration line is used.

CHAPTER 3

EXPERIMENTAL SECTION

3.1 Experiments on One Compartment Model

3.1.1 Single IV Bolus

An intravenous injection (IV bolus) ensures that a certain amount of drug is made available in the circulation instantaneously by avoiding the first pass effect. Also, the time taken to administer the drug is comparatively less [4, 5]. An IV bolus of 0.04 g is administered to the vessel.

Assumptions-

1. The distribution of the drug is instantaneous and homogenous throughout the compartment.
2. The drug introduced in the blood stream comes to a rapid equilibrium with the drug in the extra vascular tissues.
3. There is also rapid mixing; the drug mixes instantaneously with the blood. The mixing time is small when compared to the sampling time.
4. The rate of change of drug concentration is directly proportional to the drug concentration in the compartment.

Experimental Procedure-

The flow rates were adjusted until a target volume V was achieved in the central compartment. These flow rates were calibrated prior to performing the experiments using a stopwatch and a graduated cylinder. At the beginning of each experiment, 1.5-mL of

sample was taken from the beaker to the spectrophotometer (set at 530 nm) and served as a blank. The first data point was collected and its absorbance measured right after a prescribed loading dose was injected into the compartment using a transfer pipette. Similar measurements were recorded at regular time interval after 10ml of tracer was added to the central compartment. Dilutions were necessary, in some case's, to keep the absorbance readings within the range covered by a calibration line: $y = 0.0016 \times A$ where y represented the concentration in g/mL and A the absorbance.

3.1.2 Multiple IV Boluses

After a single-dose administration, the plasma drug level immediately rises above a minimum effective concentration. However, if a second dose is not taken at a specific time, the drug may not be useful as the plasma concentration drops well below the therapeutic level. Such a situation can be circumvented by prescribing a multiple-dosing regimen to the patient [7].

Multiple boluses of 0.04 g are administered to the vessel at very 60 seconds. The elimination rate constant is $0.028 \text{ second}^{-1}$. In this case, the loading dose equals the maintenance dose.

Assumptions-

The assumptions made in IV bolus still hold. In addition, the principle of superposition assumes that early doses of drug do not affect the pharmacokinetics of the subsequent doses.

Experimental Procedure-

A procedure, similar to the one adopted in the case of a single IV bolus, was used. Nine IV boluses of 0.04 g are added at an interval of 60 seconds each, the samples are collected every 15 seconds.

3.1.3 Effect of Size of Dose and Dosage Interval

There are two main parameters that can be manipulated in developing a dosage regime:

- (1) The size of the drug dose (dosage size) and
- (2) The frequency of drug administration (i.e., the time interval between doses or the dosage interval).

Studies were conducted to assess, how initial doses and drug-dosing intervals affected drug concentration in the central compartment.

In the first part of the experiment, the loading dose was 0.073 g which was later changed to 0.11 g, for 9 IV boluses. In the second part, dosing interval was changed from 45 to 30 seconds for loading doses of 0.073 g and 0.11 g. The loading dose equals the maintenance dose in all the above cases. The elimination rate constant is $0.028 \text{ second}^{-1}$ in all the above-mentioned cases.

Assumptions-

The assumptions made in the case of multiple IV boluses also apply in this study.

Experimental Procedure-

The method outlined in the case of a single IV bolus, was used. In addition, 9 IV boluses are added at an interval of 45 seconds each whereas the samples are collected every 15 seconds. This procedure is followed when studying the effects of the dosage size and administration time.

3.1.4 Effect of Time Dependent Kinetics

The elimination rate directly effects the distribution of the drug in one compartment model. In some cases depending on the duration, this may accurately explain long term clinical studies. Changes in elimination rate were reported in [9].

The loading dose is 0.17 g and elimination rate constant is 0.014 min^{-1} , which is changed at frequent intervals.

Assumptions-

In addition to the assumptions made in the previous case, the elimination rate constant changes instantaneously, with the outlet flow rate.

Experimental Procedure-

The method outlined in the case of an IV bolus, was used. In this case, a new dose is added every 45 minutes and samples are collected at an interval of 15 minutes. During the addition of a new dose, the inlet and outlet flow rates of water are changed simultaneously to maintain the liquid level in the beaker.

3.1.5 Infusion

The main advantage for administering a drug by IV infusion is that IV infusion allows precise control of plasma drug concentrations to fit the individual needs of the patient. For drugs with a narrow therapeutic window, IV infusion maintains an effective constant plasma drug concentration by eliminating wide fluctuations. Furthermore, the duration of drug therapy may be maintained or terminated as needed using IV infusion. To reach a MEC, a bolus dose requires some time to be completely diluted in blood and hence, slow infusion is preferred [5].

Assumptions-

The assumptions made in the multiple IV cases still hold.

Experimental Procedure-

The method outlined in the case of a multiple IV boluses, was used. However, in this case the infusion was started at $t = 0$ and samples were collected at an interval of 15 minutes.

3.1.6 IV Bolus and Infusion

The time taken by the drug to reach a steady-state value is very long with IV Infusion. To circumvent this problem, multiple boluses are often used prior to initiate a constant-rate infusion. This experiment is conducted in two parts:

- (a) One compartment model with infusion and one IV bolus
- (b) One compartment model with infusion and multiple IV boluses.

The experiment was carried out to achieve a steady-state value of 0.36 g in the compartment with $k_{el} = 0.014 \text{ min}^{-1}$ and $k_o = 5.6 \text{ g/min}$.

Assumptions-

The assumptions made in the multiple IV cases were applied.

Experimental Procedure-

For part (a) at time $t = 0$ the flow of drug into the compartment began at the same time an bolus of 0.4 g was added, whereas for part (b) of the experiment, two cases were used: two IV boluses in one case and four IV boluses in another case, both combined with an infusion. A loading dose, (equivalent to the maintenance dose) of 0.4 g was used. The aim of the study was to find out which of the two cases showed the best performance.

3.2 Experiments on Two Compartment Model

3.2.1 Single IV Bolus

A two-compartment model gives a good representation of the human body, where the central compartment represents the blood and the peripheral compartment represents the tissues [11].

An IV bolus of 1.37 g is administered to the central compartment.

Assumptions-

The assumptions made in the previous cases still apply.

Experimental Procedure-

The method outlined in the case of a single IV bolus, was used.

3.2.2 Multiple IV Boluses

The administration of a single bolus will cause the plasma drug concentration to fall below the MEC. To avoid such a situation, a second bolus has to be administered [4]. In order to develop a drug administration regime with multiple boluses for a two-compartment model. The kinetic rate constants should be known. These kinetic rate constants define the transport between both compartments [14].

A drug administration regime has been developed with three IV boluses having a loading dose of 0.82 g. The first and last maintenance doses are 0.314 g and 0.242 g respectively. The kinetic rate constants are the same as in those used in the previous experiment: $k_{12} = 1.7999 \text{ hr}^{-1}$, $k_{21} = 2.9246 \text{ hr}^{-1}$ and $k_{el} = 0.2739 \text{ hr}^{-1}$.

Assumptions-

The assumptions made in the previous cases still apply.

Experimental Procedure-

The method outlined in the case of a single IV bolus in a two-compartment model was used. The samples were collected at an interval of 15 minutes for both the central and the peripheral compartments. The first and the second maintenance dose were added to the central compartment at 90 minutes and 180 minutes, respectively.

3.2.3 Effect of Time Dependent Kinetics

The kinetic rate constants play a very important role in determining the elimination of the drug from the central compartment as well as the transport of the drug between the two compartments. A change in any of these constants effects the drug distribution.

There are three rate constants, k_{12} , k_{21} and k_{el} , which are identified in the setup. The kinetic rate constant k_{12} is responsible for the transport of drug from the central to the peripheral compartment, whereas the kinetic rate constant k_{21} is responsible for the transport of drug from the peripheral to the central compartment. The kinetic rate constant k_{el} is responsible for the elimination of the drug from the central compartment. Changes are made to one rate constant, keeping the other two constant. The effects of the time dependent kinetics are studied.

Assumptions-

The assumptions made in the previous case were applied. In addition, it is assumed that the elimination rate constant changes instantaneously, with the flow rate of the outlet stream.

Experimental Procedure-

The method outlined in single IV bolus in two-compartment model, was used. The flow rates governing the kinetic rate constants are changed, prior to adding the KMnO_4 solution.

3.2.4 Infusion

The main advantage for giving a drug by IV infusion is that this method allows precise control of the plasma drug concentrations. The drug is infused in the central compartment where it is eliminated and also transported into the peripheral compartment. The desired effect is observed in the central compartment [16].

A drug administration regime has been developed to maintain 0.695 g of drug in the central compartment. The kinetic rate constants used in the experiment are $k_{12} = 1.0968 \text{ hr}^{-1}$, $k_{21} = 2.3596 \text{ hr}^{-1}$ and $k_{el} = 1.4335 \text{ hr}^{-1}$.

Assumptions-

The assumptions made in the previous case still hold.

Experimental Procedure-

The method outlined for a single IV Bolus in two-compartment model was used. The samples were collected at an interval of 15 minutes for both the central and the peripheral compartment. The infusion is started at time $t = 0$.

3.2.5 IV Boluses with Infusion

Drug administration by IV infusion is very effective since there is precise control over the plasma drug concentration. It is also possible to maintain the drug concentration within a specific range. The time taken by the drug to reach the effective level is generally very

high during infusion. This time could be reduced by administering IV boluses as suggested in [18].

A drug dosage regime was developed with a loading dose of 0.808 g and two maintenance doses of 0.201 g and 0.196 g coupled with infusion rate of 0.996 g/hr, where the infusion is started at $t = 0.5$ hr.

Assumptions-

The assumptions made in the previous case still hold.

Experimental Procedure-

The method outlined in the case of multiple IV Boluses is used. A loading dose of 0.808 g is given at time $t = 0$ and two maintenance doses of 0.201 g and 0.196 g were respectively given at time $t = 0.12$ hour and $t = 0.254$ hour. The infusion is started at time $t = 0.5$ hours.

CHAPTER 4

RESULTS AND DISCUSSIONS

4.1 Experiments on One Compartment Model

4.1.1 Single IV Bolus

A sample is taken every 30 seconds. The concentration profile is exponentially decreasing which can be seen from Figure 4.1. It can also be concluded that if multiple boluses were to be injected, the next bolus should be between 40 and 60 seconds after the first bolus has been administered for the same loading dose. The data analysis as discussed in Appendix C.1 which yields an elimination rate of $0.028 \text{ second}^{-1}$. This value of the elimination rate is used for future experiments with one compartment model.

The sum of the squared difference between the experimental and the calculated profile is very small. The concentration profile obtained for the drug is very similar to the concentration profile obtained for Nafcillin in [6] is as shown in Figure 4.2.

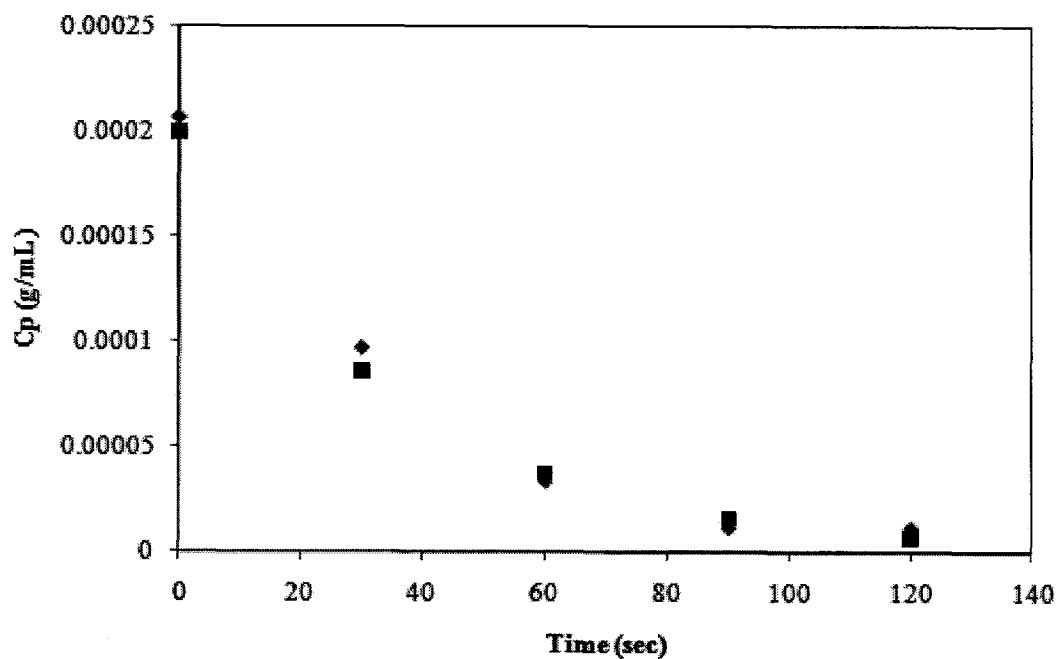


Figure 4.1 Plasma drug concentration-time profile for a single bolus dose. Loading dose is 0.04 g, $k_{el} = 0.028 \text{ second}^{-1}$. The symbols (\diamond) represent the experimental profile and (\blacksquare) represent the calculated profile.

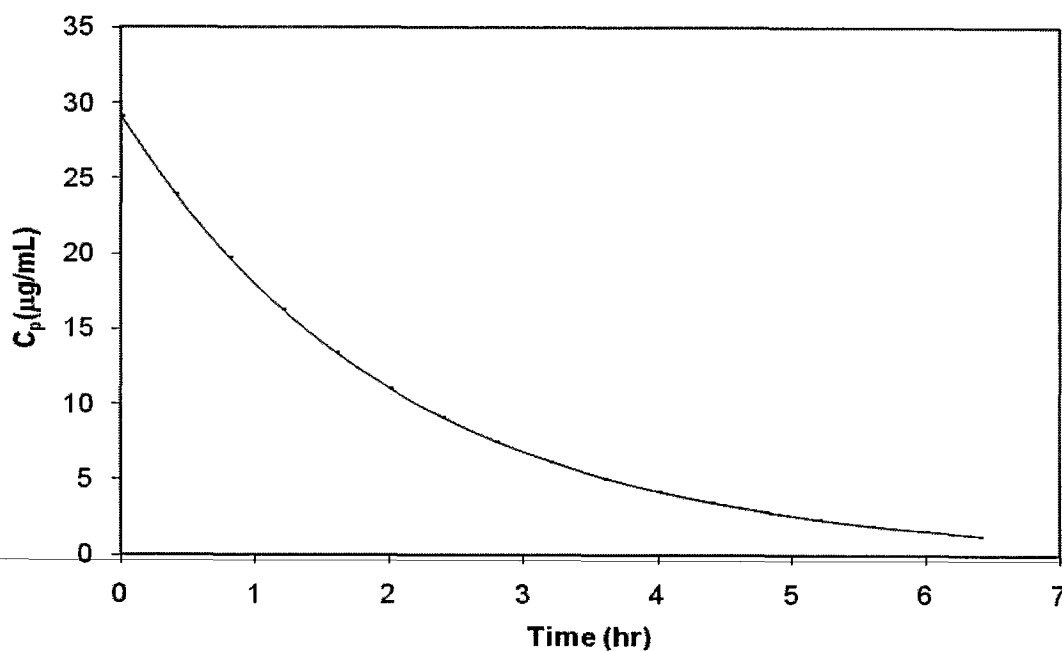


Figure 4.2 Plasma concentration profile due to one IV bolus (Nafcillin) : $C_p^0 = 29.1 \mu\text{g/mL}$, $k_{el} = 0.483 \text{ hr}^{-1}$.

4.1.2 Multiple IV Boluses

During repeated drug administration, the concentration profile will be repeated for each dosage interval [8]. 9 IV boluses are given in the experiment. The experimental data is shown below in Figure 4.3, whereas the calculated data are shown in Figure 4.4. The concentration profile obtained experimentally is very similar to the concentration profile for Nafcillin in [6] as shown in Figure 4.5.

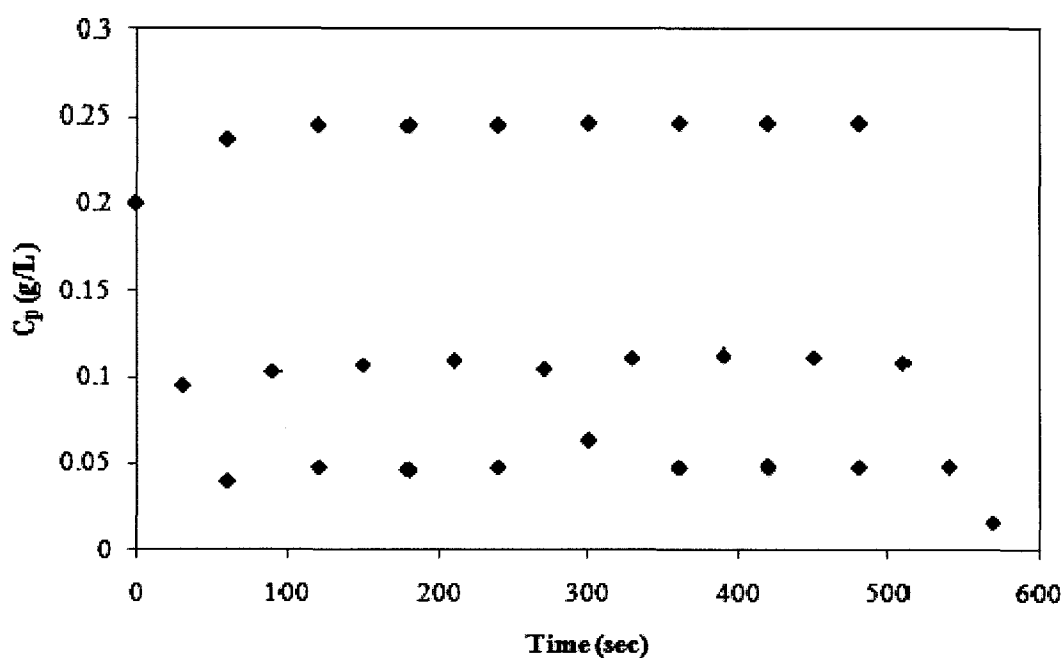


Figure 4.3 Plasma drug concentration time profile for a one compartment model with nine IV Boluses. Loading dose is 0.04 g, $k_{el} = 0.028 \text{ second}^{-1}$, $n = 9$ and $\tau = 60 \text{ second}$. The symbols (♦) represent the experimental profile.

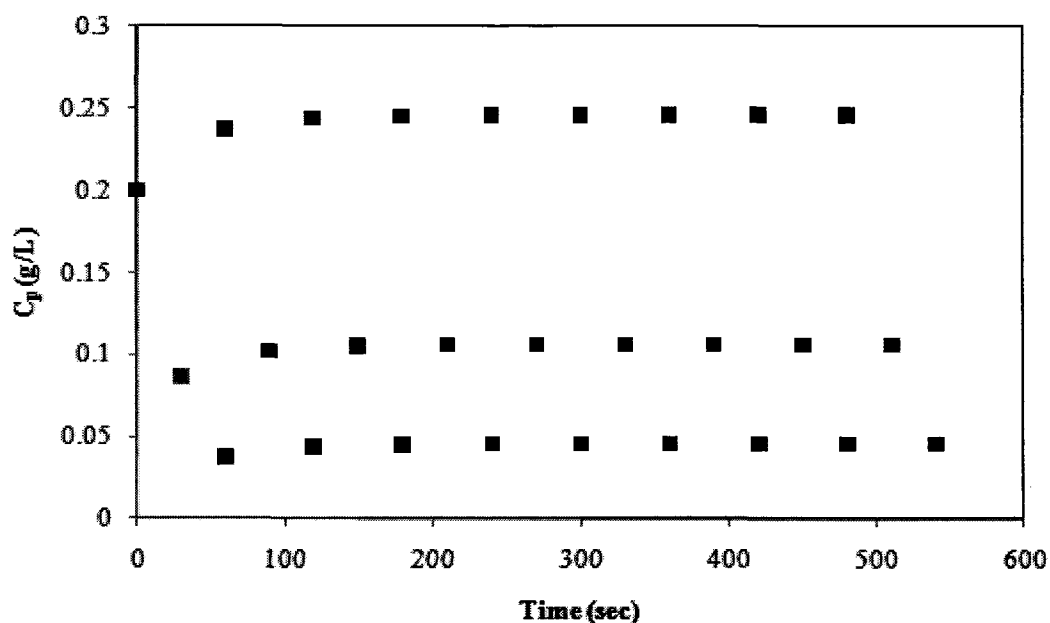


Figure 4.4 Theoretically calculated plasma drug concentration time profile for one compartment model with nine IV Boluses. Loading dose is 0.042 g, $k_{el} = 0.028 \text{ second}^{-1}$, $n = 9$ and $\tau = 60 \text{ sec}$. The symbols (■) represent the calculated profile.

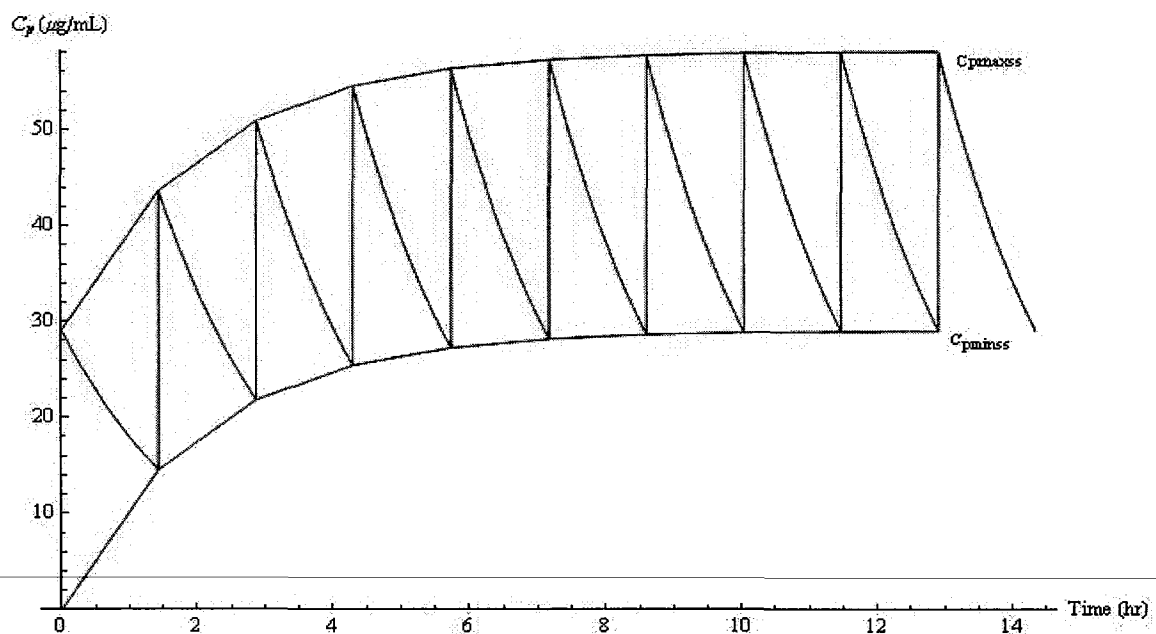


Figure 4.5 Plasma concentration profile for a multiple IV bolus regimen. The parameters for nafcillin, $C_p^0 = 29.1 \text{ μg/mL}$ and $k_{el} = 0.483 \text{ hr}^{-1}$. For the simulation, $n = 10$ and $\tau = t_{1/2}$.

The C_{pmax} and the C_{pmin} values reached during the experiment are respectively 0.24645 g/L and 0.0477 g/L, whereas theoretical C_{pmax} and the C_{pmin} values obtained are respectively 0.24623 g/L and 0.04589 g/L. The sum of the squared difference between the calculated profile and the profile obtained experimentally is 0.0007.

4.1.3 Effect of Size of Dose and Dosage Interval

Part 1 of the experimental results obtained is shown in Figure 4.6. Each drug has a toxic level and a non effective level in the human body. When the drug is administered into the human body, it should not exceed the MTC so as not to become harmful and should not fall below MEC. As a result, C_{pmax} and the C_{pmin} are within MTC and MEC. Using this information, coupled with the desired maximum and minimum concentration, the dose interval can be decided. The values obtained experimentally are very close to the theoretical values.

These findings suggest that the two doses leads to a different maximum and minimum. The number of doses required to reach a steady cycle is the same because there is no change in the dose interval.

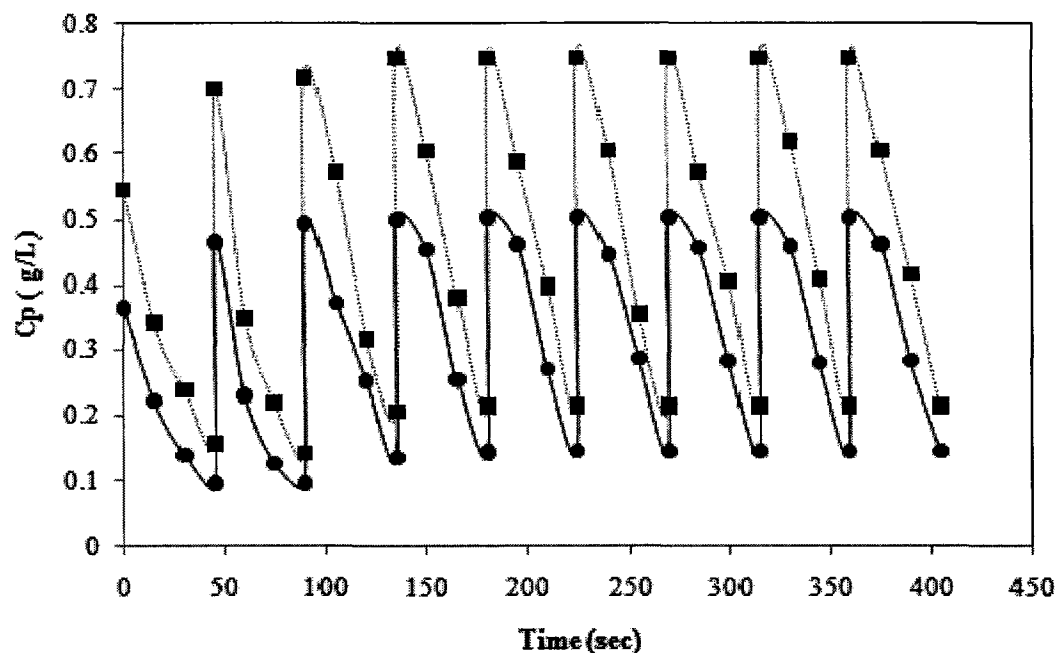


Figure 4.6 Plasma drug concentration time profile for one compartment model with nine IV Boluses with two drug sizes. Here, Dose # 1 is 0.073 g represented by (●) and Dose # 2 is 0.109 g represented by (■), $k_{el} = 0.028 \text{ second}^{-1}$ for both and $\tau = 45$ seconds.

For the second part of the experiment, the dosage interval is changed from 45 seconds to 30 seconds. The results are shown in Figure 4.7 and Figure 4.8. Since the dosage interval is changed for both loading dose's, it can be seen that a new higher maximum and minimum values are obtained at $\tau = 30$ seconds which are higher than the values obtained when $\tau = 45$ seconds. The change in dosage interval has a profound impact on the distribution regime. If the dosage interval is shortened, higher maximum and minimum levels will be obtained. The profile observed during multiple IV boluses mimic a infusion for very short administration time.

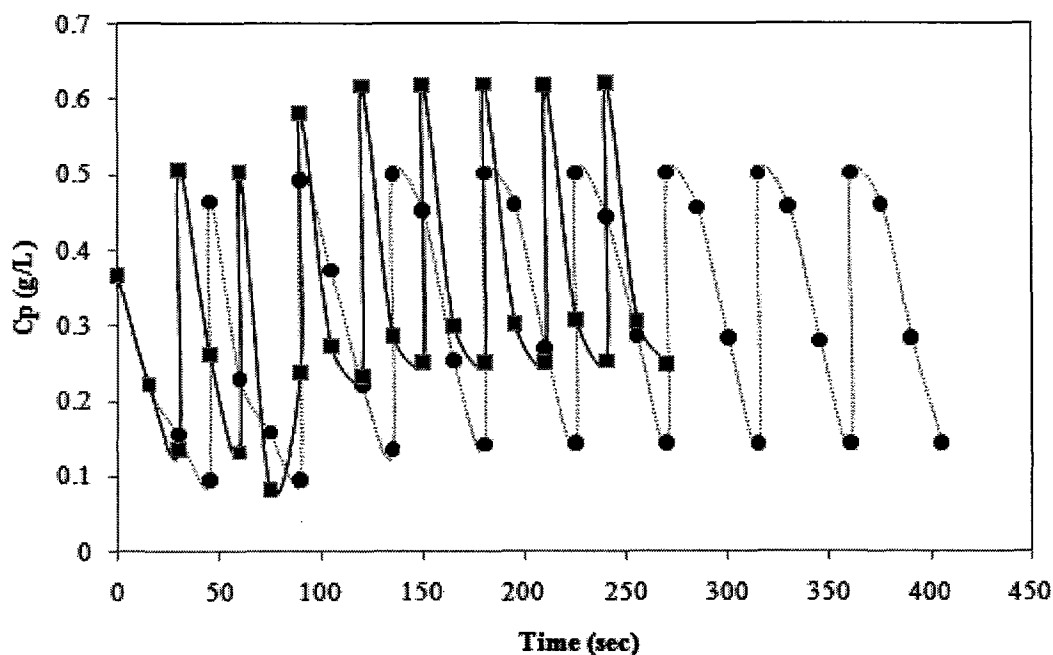


Figure 4.7 Plasma drug concentration time profile for the change in dose interval. Dose # 1 = 0.073 g, $k_{el} = 0.028 \text{ second}^{-1}$ for $\tau = 45 \text{ sec}$ (●) and $\tau = 30 \text{ sec}$ (■).

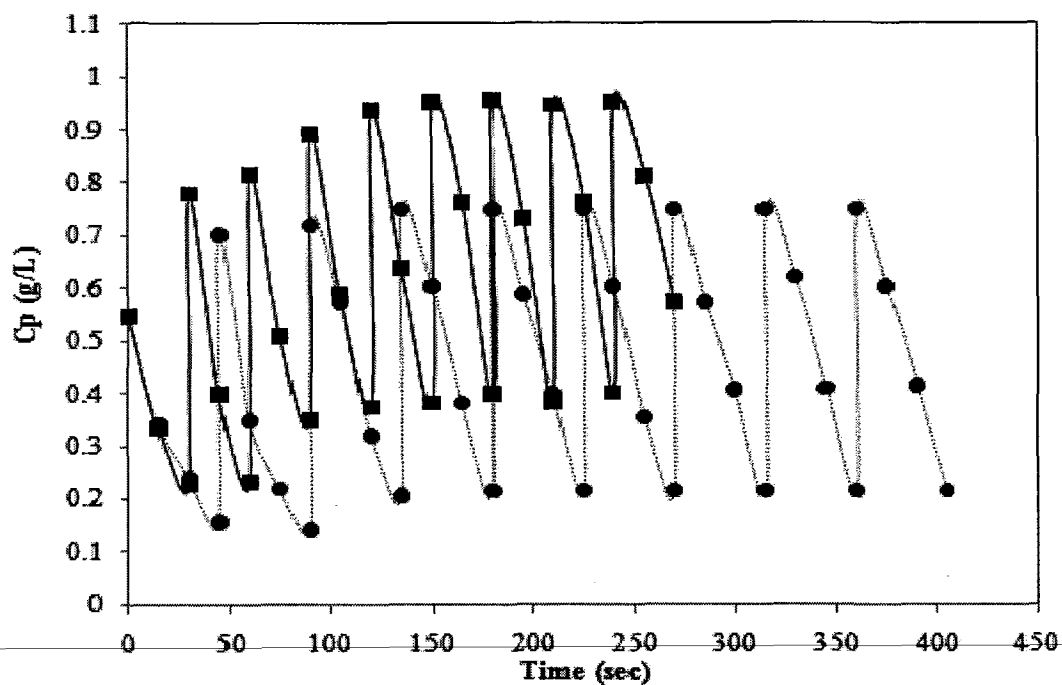


Figure 4.8 Plasma drug concentration time profile for the change in dose interval. Dose # 2 = 0.109 g, $k_{el} = 0.028 \text{ second}^{-1}$ for $\tau = 45 \text{ sec}$ (●) and $\tau = 30 \text{ sec}$ (■).

4.1.4 Effect of Time Dependent Kinetics

The change in the elimination rate is shown graphically in Figure 4.9 and the concentration profile of the drug when the elimination rate is changed during the addition of a new dose is shown in Figure 4.10.

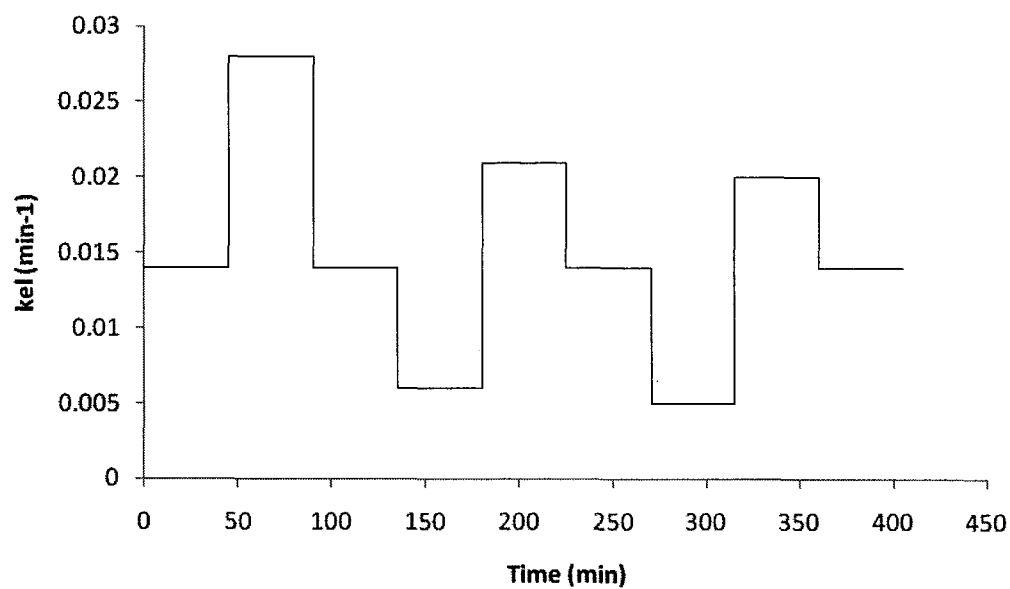


Figure 4.9 Change of the rate constant of elimination during the length of the experiment.

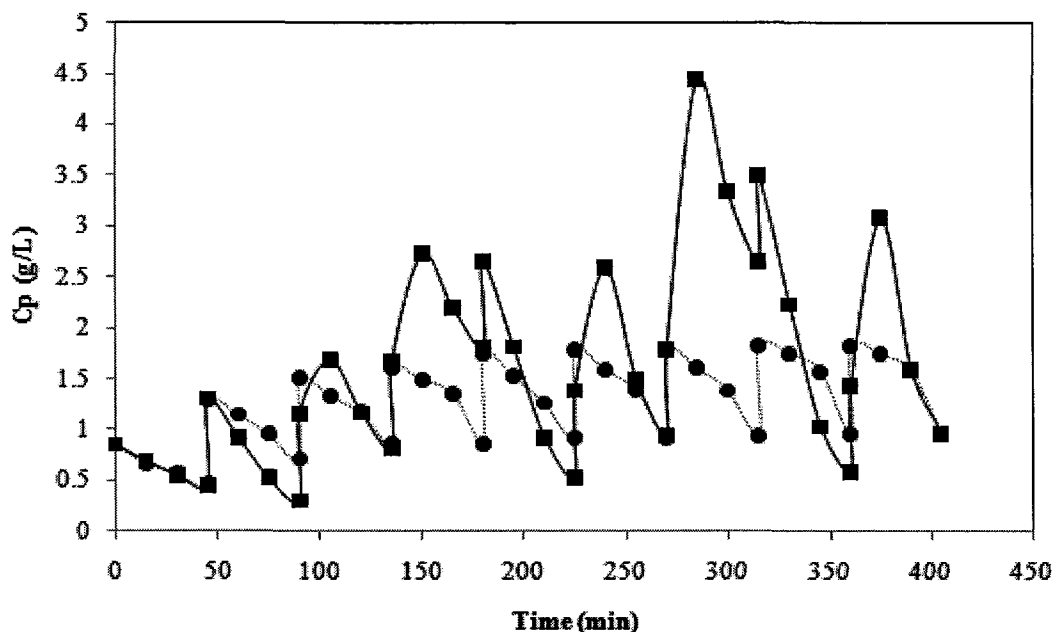


Figure 4.10 The comparison between the plasma drug concentration time profiles with a constant $k_{el} = 0.014 \text{ minute}^{-1}$ (●) and a plasma drug concentration time profile with varying k_{el} (■). Loading dose = 0.169 g and $\tau = 45$ min.

Figure 4.10 provides a comparison between the 1st case where the elimination constant remains at 0.014 min^{-1} and the 2nd case where the k_{el} changes during the experiment. The concentration profiles are similar for both cases as the k_{el} values are the same.

Before the second dose is administered the k_{el} value has been changed to 0.028 min^{-1} which is higher than that of the first dose, so the maximum concentration reached by both cases are the same but the minimum concentration reached is lower.

The third dose in both the cases, have the same k_{el} value but the maximum values attained are different, as the minimum value attained for the 2nd dose is lower and hence when the third dose is added the maximum reached is lower than that achieved in the 1st case.

The fourth dose is introduced at a very low k_{el} ($k_{el} = 0.006 \text{ min}^{-1}$) value in the 2nd case. The maximum values reached at 135 minutes are also the same for both the cases. However, more accumulation is observed in the 2nd case due to the low k_{el} value. As a result, the concentration of KMnO_4 is higher in the 2nd case than the 1st case when $t = 150 \text{ min}$.

The fifth dose is introduced at a higher k_{el} ($k_{el} = 0.021 \text{ min}^{-1}$) value in the 2nd case. As the fourth dose was at a very low k_{el} value the minimum reached is very high compared to that of the fourth dose in the 1st case, so the maximum value for the fifth dose is higher in the 2nd case. Also, the minimum reached is lower for the fifth dose in the 2nd case when compared to the fifth dose in the 1st case.

The k_{el} values are the same for the sixth dose. Since the minimum reached for the fifth case in the 2nd case was lower than that of the 1st, the maximum reached for the sixth dose is higher for the 1st case. As the value of k_{el} for the 2nd case decreased from 0.021 min^{-1} to 0.014 min^{-1} there is accumulation of KMnO_4 which is shown by the sample at 240 minutes. The minimum achieved for both cases are similar. Similar trends are observed for the remaining doses.

Change in k_{el} can severely affect the concentration profile of the drug in the body. The increase in k_{el} values leads to the faster removal of drug from the system; the drug may then drop below the effective level. The decrease in k_{el} values leads to the slower removal of drug from the system; the drug may accumulate in such amounts as to cross the toxic level and become harmful for the body.

If the k_{el} value changes in the course of treatment, the drug may reach a value that is harmful to the patient. The development of drug regimen in accordance with changing

k_{el} is very difficult as there is no method to determine how k_{el} will change and correspondingly how it will affect the plasma drug concentration.

4.1.5 Infusion

During constant-rate infusion, the concentration increases exponentially. When the infusion is stopped, the amount of drug decreases [10]. Experimental and predicted time concentration profiles are shown in Figures 4.11 and 4.12, respectively. A similar trend is observed for the constant rate infusion of Ampicillin Trihydrate in [5]. The sum of the squared difference between the calculated profile and the experimentally obtained profile is 0.004329. The time it takes to reach the steady state value of 0.4 g is 165 minutes.

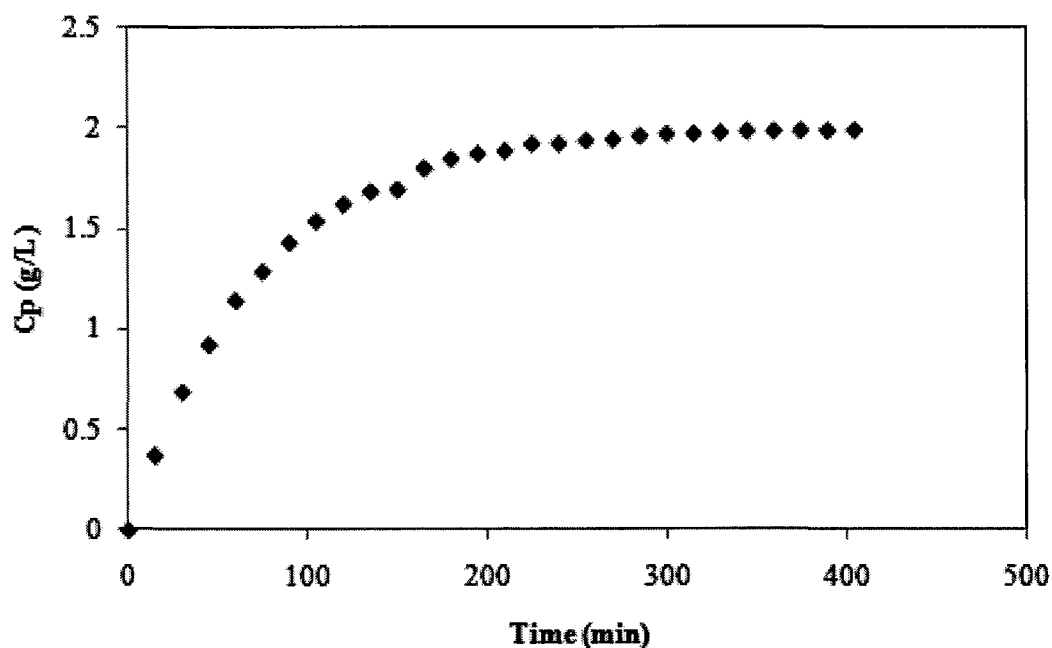


Figure 4.11 The symbols (♦) represent the experimental concentration profile for $k_{el} = 0.014 \text{ min}^{-1}$ and $k_0 = 5.6 \text{ g/min}$.

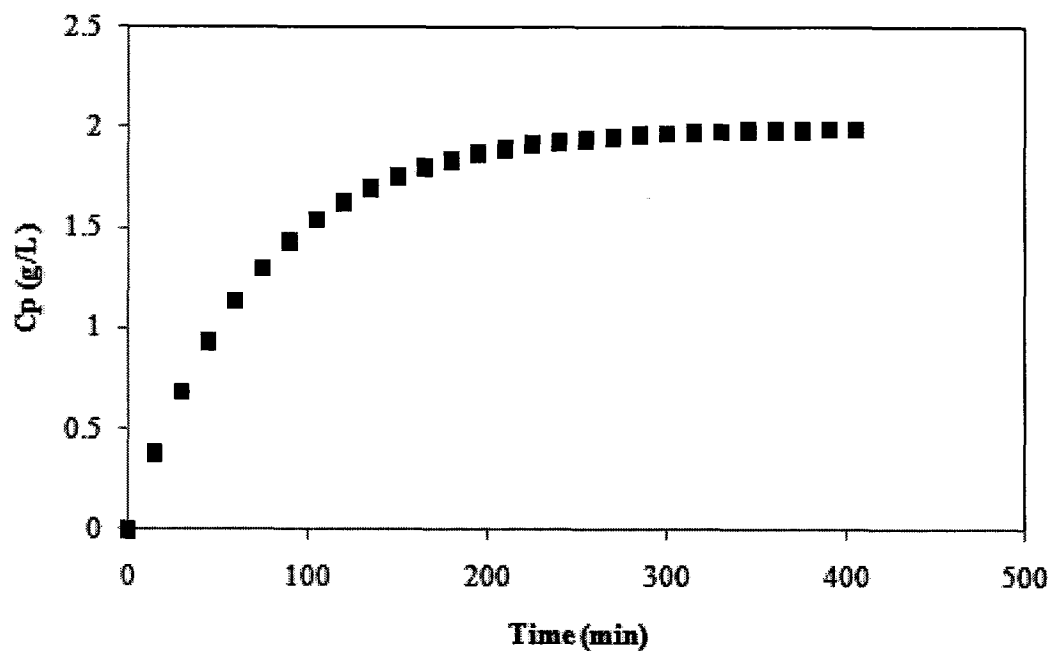


Figure 4.12 Calculated concentration profile is represented by the symbols (■) for $k_{el} = 0.014 \text{ min}^{-1}$ and $k_o = 5.6 \text{ g/min}$.

4.1.6 IV Boluses and Infusion

The concentration profile for one IV bolus with Infusion is shown in Figure 4.13, the results for four and two IV boluses with Infusion are shown in Figure 4.14.

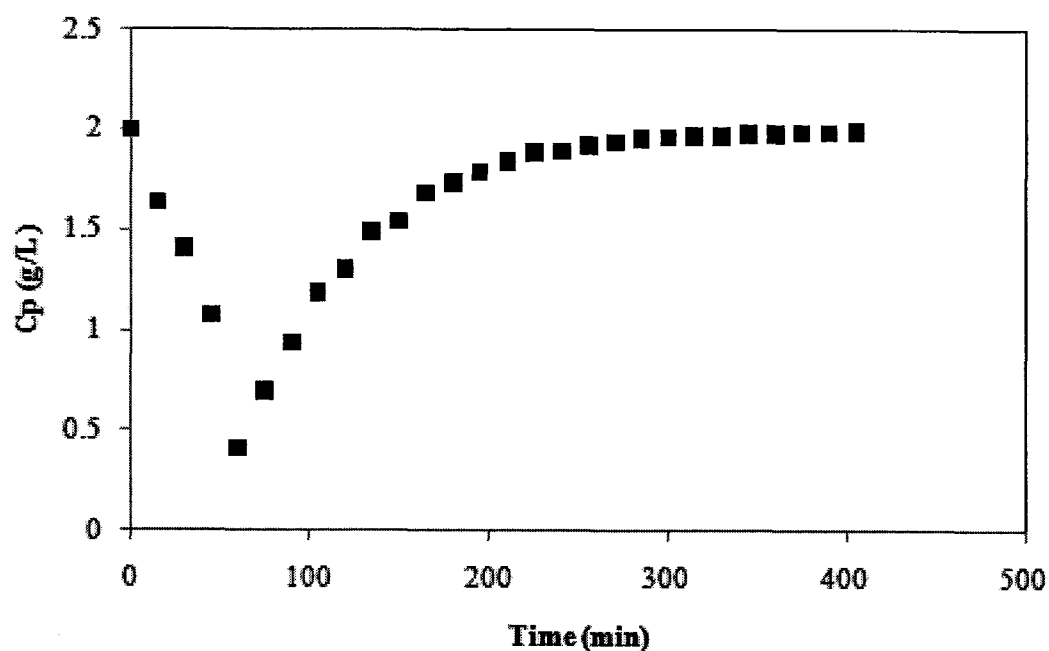


Figure 4.13 Plasma concentrations versus time for one IV bolus with infusion are represented by (■), with loading dose of 0.4 g, $k_{el} = 0.014 \text{ min}^{-1}$ and $k_0 = 5.6 \text{ g/min}$.

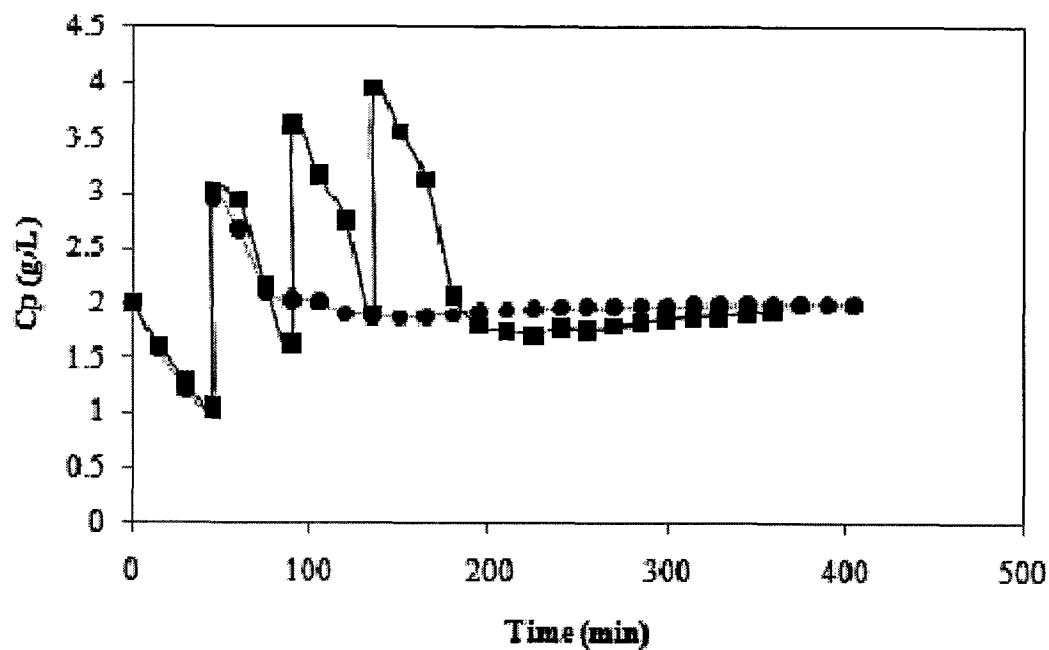


Figure 4.14 Plasma concentrations versus time for two (●) and four IV boluses (■) with loading dose as 0.4 g and $k_{el} = 0.014 \text{ min}^{-1}$ followed by a constant-rate infusion of $k_0 = 5.6 \text{ g/min}$.

Part (a)

From Figure 4.13, it can be concluded that one IV bolus is not sufficient for the compartment to achieve a steady state value of 2 g/L quickly through the infusion. To lessen the time it takes to reach the steady state value, two boluses with infusion and four boluses with infusion are tested. The sum of the squared difference between the calculated profile and the profile obtained experimentally is 0.8332.

Part (b)

In the experiment of four IV Boluses with IV Infusion the concentration of the drug reaches a very high value. It is possible for the system to reach steady state value with lower number of IV boluses as the minimum concentration reached after two boluses is nearer to the steady state value of 2 g/L. Experiment with two IV boluses with Infusion is conducted. A response time of 120 minutes was recorded. The sum, of the squared difference between the calculated profile and the profile obtained experimentally for two IV boluses with infusion is 0.1179, and for four IV boluses with infusion is 0.1322.

4.2 Experiments using Two Compartment Model**4.2.1 Single IV Bolus**

The experimental and calculated concentration profiles for two compartment model are shown in Figure 4.15 Figure 4.16, respectively.

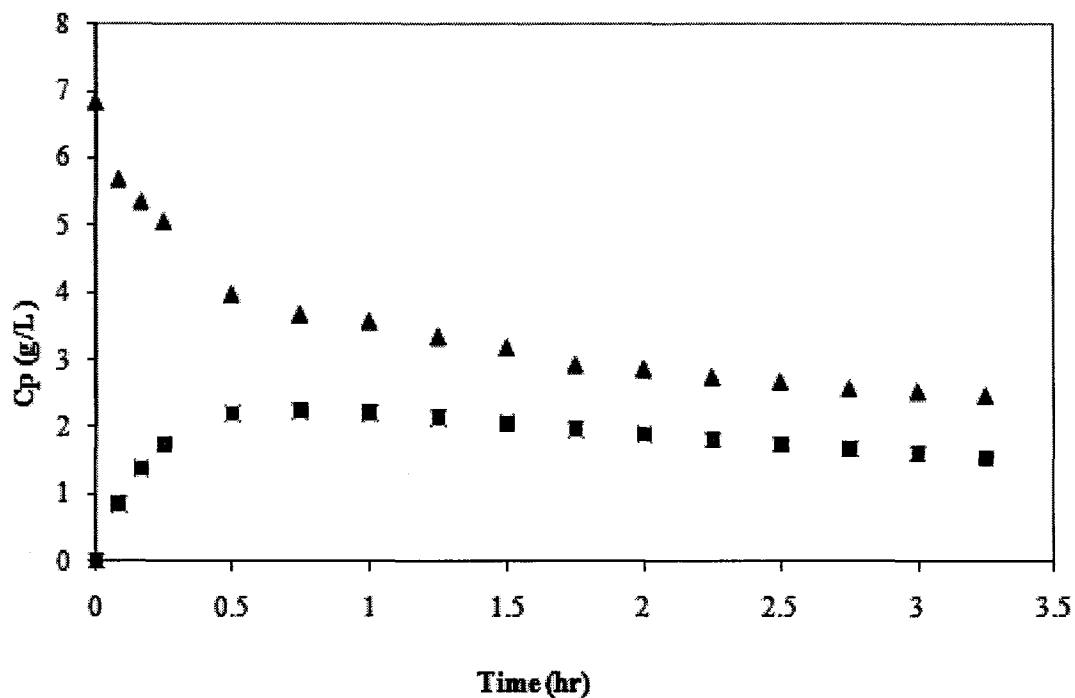


Figure 4.15 Concentration profile for two-compartment model with initial dose 1.37 g. The symbols (\blacktriangle) and (\blacksquare) represent the profile for the central and peripheral compartment, respectively.

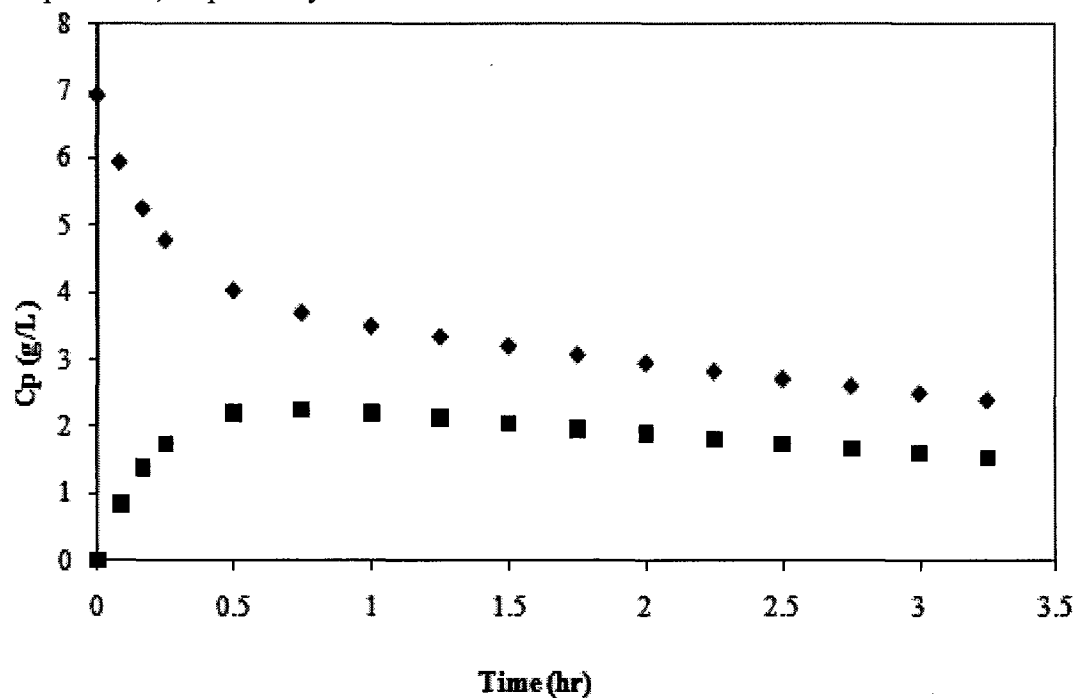


Figure 4.16 Calculated concentration profile for two compartment model, with a initial dose of 1.37 g. The symbols (\blacklozenge) and (\blacksquare) represent the profile for the central and peripheral compartment respectively.

The sum of the squared difference between the calculated profile and the profile obtained experimentally is 0.17 for the central compartment and 0.000545 for the peripheral compartment. The data was analyzed using a method similar to that adopted in [12]. Details are provided in Appendix C.2. The estimated values of the kinetic rate constants obtained after data analysis are $k_{12} = 1.7999 \text{ hr}^{-1}$, $k_{21} = 2.9246 \text{ hr}^{-1}$ and $k_{el} = 0.2739 \text{ hr}^{-1}$. The concentration profile in the central compartment is similar to the one described in [13].

4.2.2 Multiple IV Boluses

Experimental and predicted concentration profiles are shown in Figures 4.17 and 4.18, respectively. The predicted values obtained using the code is outlined in Appendix D.1.

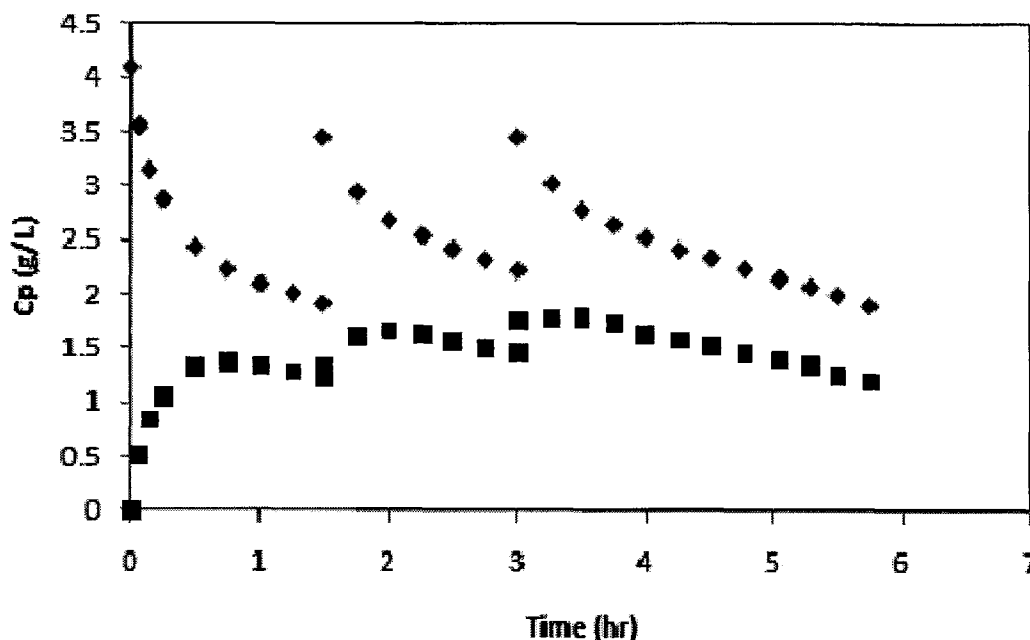


Figure 4.17 Concentration profile for multiple boluses, with a loading dose of 0.82 g. The first and second maintenance doses are 0.314 g and 0.252 g, respectively. The kinetic rate constants are $k_{12} = 1.7999 \text{ hr}^{-1}$, $k_{21} = 2.9246 \text{ hr}^{-1}$ and $k_{el} = 0.2739 \text{ hr}^{-1}$. The symbols (◆) and (■) represent the profile for the central and peripheral compartment respectively.

The sum of the squared difference between the calculated profile and the profile obtained experimentally is 0.14 for the central compartment and 0.217 for the peripheral compartment. The dosage regime developed is very close to that obtained experimentally.

A similar trend for multiple boluses is observed in [15].

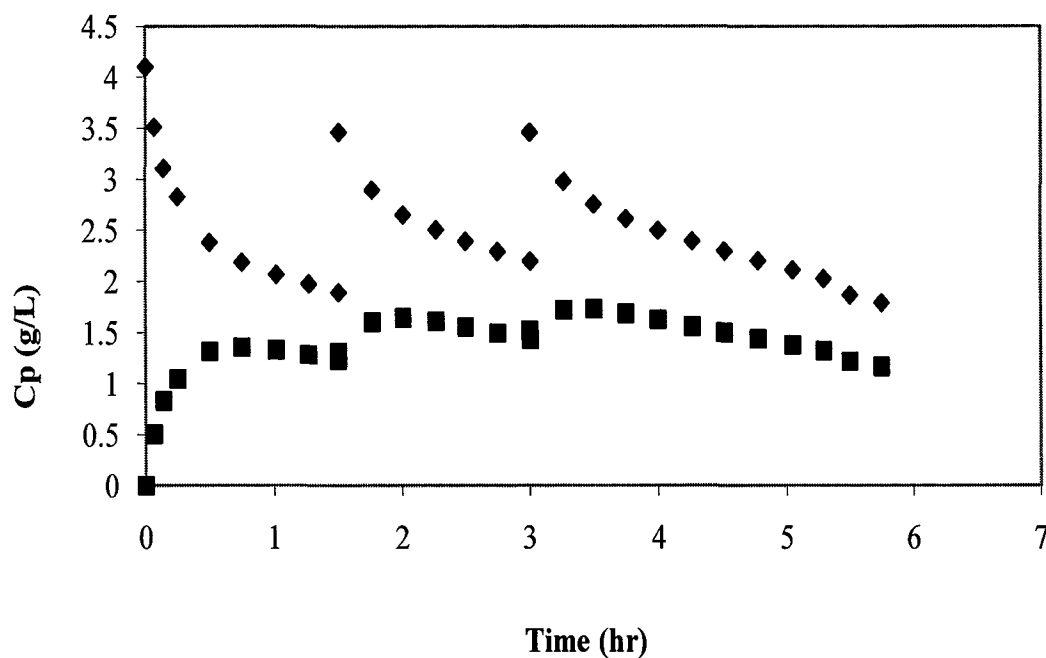


Figure 4.18 Calculated concentration profile for multiple boluses, with loading dose of 0.82 g. The first and second maintenance doses are 0.314 g and 0.252 g, respectively. The kinetic rate constants are $k_{12} = 1.7999 \text{ hr}^{-1}$, $k_{21} = 2.9246 \text{ hr}^{-1}$ and $k_{el} = 0.2739 \text{ hr}^{-1}$.

4.2.3 Effect of Time Dependent Kinetics

The experiment has been conducted in three parts, (1) changing k_{12} from 1.7993 hr^{-1} to 1.4023 hr^{-1} while keeping k_{21} and k_{el} constant, (2) changing k_{21} from 2.9246 hr^{-1} to 3.7948 hr^{-1} while keeping k_{12} and k_{el} constant and (3) changing k_{el} from 0.2739 hr^{-1} to 0.4129 hr^{-1} while keeping k_{12} and k_{21} constant.

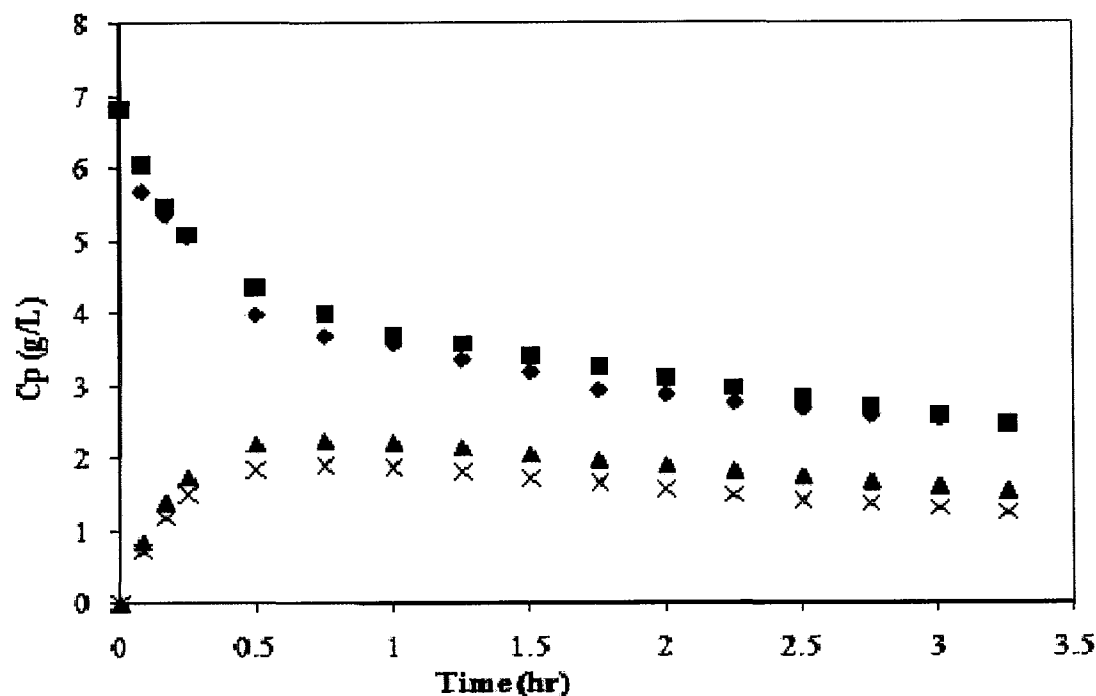


Figure 4.19 Concentration profile for one IV bolus of 1.37 g, where the symbols (♦) and (▲) represent the profile for the central and peripheral compartment respectively. The kinetic rate constants are $k_{12} = 1.7993 \text{ hr}^{-1}$, $k_{21} = 2.9246 \text{ hr}^{-1}$ and $k_{el} = 0.2739 \text{ hr}^{-1}$. Where as the symbols (■) and (X) represent the profile for central and peripheral compartment, respectively. The kinetic rate constants are $k_{12} = 1.4023 \text{ hr}^{-1}$, $k_{21} = 2.9954 \text{ hr}^{-1}$ and $k_{el} = 0.2815 \text{ hr}^{-1}$. The standard deviation for kinetic rate constants k_{12} , k_{21} and k_{el} are 0.291, 0.617 and 0.098, respectively.

In (1), k_{12} was reduced from 1.7993 hr^{-1} to 1.4023 hr^{-1} . The transport of drug from the central to the peripheral compartment is decreased. Hence, there is more accumulation in the central compartment and also the amount of drug in the peripheral compartment has decreased when compared to the original profile as there is lesser amount of drug being transported from the central compartment (Figure 4.19).

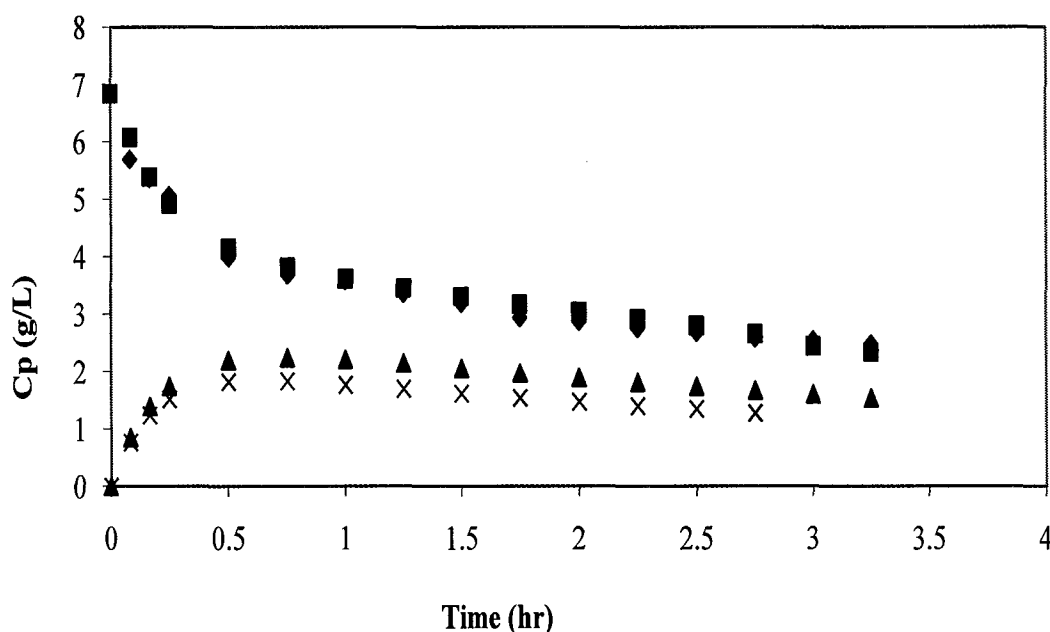


Figure 4.20 Concentration profile for one IV bolus of 1.37 g, the symbols (◆) and (▲) represent the profile for the central and peripheral compartment respectively. The kinetic rate constants as $k_{12} = 1.7993 \text{ hr}^{-1}$, $k_{21} = 2.9246 \text{ hr}^{-1}$ and $k_{el} = 0.2739 \text{ hr}^{-1}$. Whereas the symbols (■) and (X) represent the profile for central and peripheral compartment respectively. The kinetic rate constants as $k_{12} = 1.6915 \text{ hr}^{-1}$, $k_{21} = 3.7948 \text{ hr}^{-1}$ and $k_{el} = 0.2794 \text{ hr}^{-1}$.

In (2), k_{21} was increased from 2.9246 hr^{-1} to 3.7948 hr^{-1} . The transport of drug from the peripheral to the central compartment is increased. Hence there is more accumulation in the central compartment. The amount of drug in the peripheral compartment decreased when compared to the original profile as the amount of drug being transported to the central compartment increased (Figure 4.20).

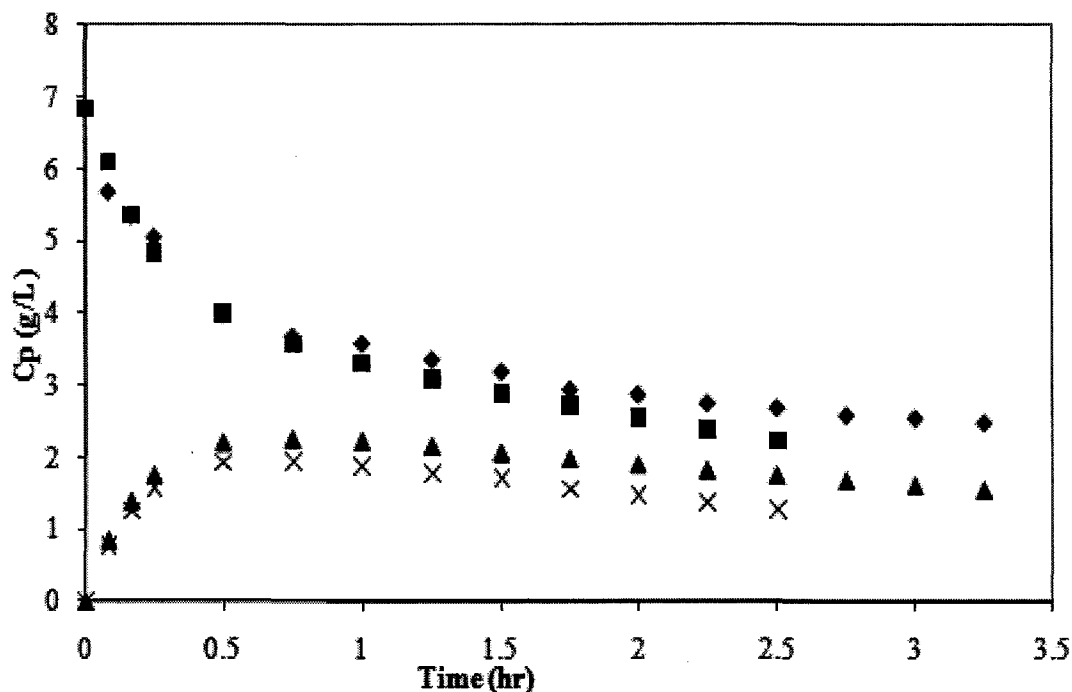


Figure 4.21 Concentration profile for one IV bolus of 1.37 g, the symbols (♦) and (▲) represent the profile for the central and peripheral compartment respectively. The kinetic rate constants as $k_{12} = 1.7993 \text{ hr}^{-1}$, $k_{21} = 2.9246 \text{ hr}^{-1}$ and $k_{el} = 0.2739 \text{ hr}^{-1}$. Whereas the symbols (■) and (X) represent the profile for central and peripheral compartment respectively. The kinetic rate constants as $k_{12} = 1.6566 \text{ hr}^{-1}$, $k_{21} = 3.0903 \text{ hr}^{-1}$ and $k_{el} = 0.4129 \text{ hr}^{-1}$.

In (3), k_{el} was increased from 0.2739 hr^{-1} to 0.4129 hr^{-1} . More drug was being eliminated for the central compartment. A decrease in the accumulation of the drug in the central compartment was observed. The amount of drug in the peripheral compartment decreased when compared to the original profile as the amount of drug being transported from the central compartment has decreased (Figure 4.21).

4.2.4 Infusion

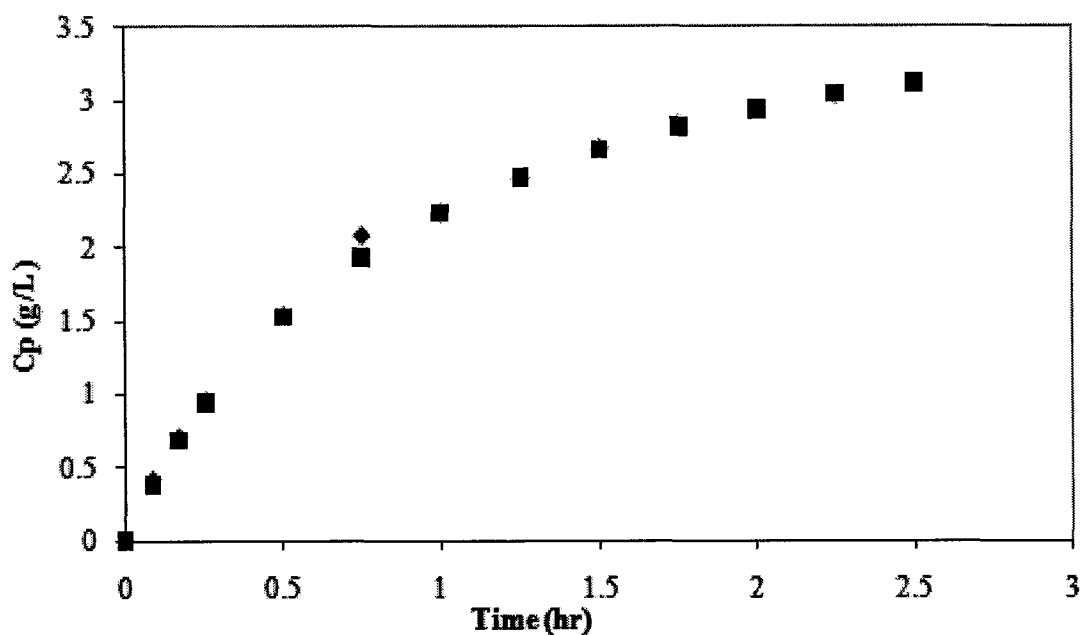


Figure 4.22 Concentration profile for IV infusion of 0.695 g of drug having an infusion rate $R = 0.996$ g/hr. The kinetic rate constants are $k_{12} = 1.0968$ hr⁻¹, $k_{21} = 2.3596$ hr⁻¹ and $k_{el} = 1.4335$ hr⁻¹. Here, the symbols (♦) represent the experimental profile and (■) represents the calculated profile.

The drug administration regime was developed to maintain a concentration of 3.46 g/L in the central compartment. The equilibrium should be reached after 6.75 hours. The experiment was conducted for 2.5 hours and it is found that the experimental plasma concentration profile closely follows the designed plasma concentration profile. The sum of the squared difference between the calculated profile and the profile obtained experimentally is about 0.0266. Figure 4.22 shows both the experimental and the calculated concentration profile.

The introduction of IV boluses with IV infusion will reduce the time required to reach the equilibrium [17].

4.2.5 IV Boluses with Infusion

The kinetic rate constants used in the experiment are $k_{12} = 1.0968 \text{ hr}^{-1}$, $k_{21} = 2.3596 \text{ hr}^{-1}$ and $k_{el} = 1.4335 \text{ hr}^{-1}$. Refer to Appendix D.2 for the code used to calculate the dosage regime.

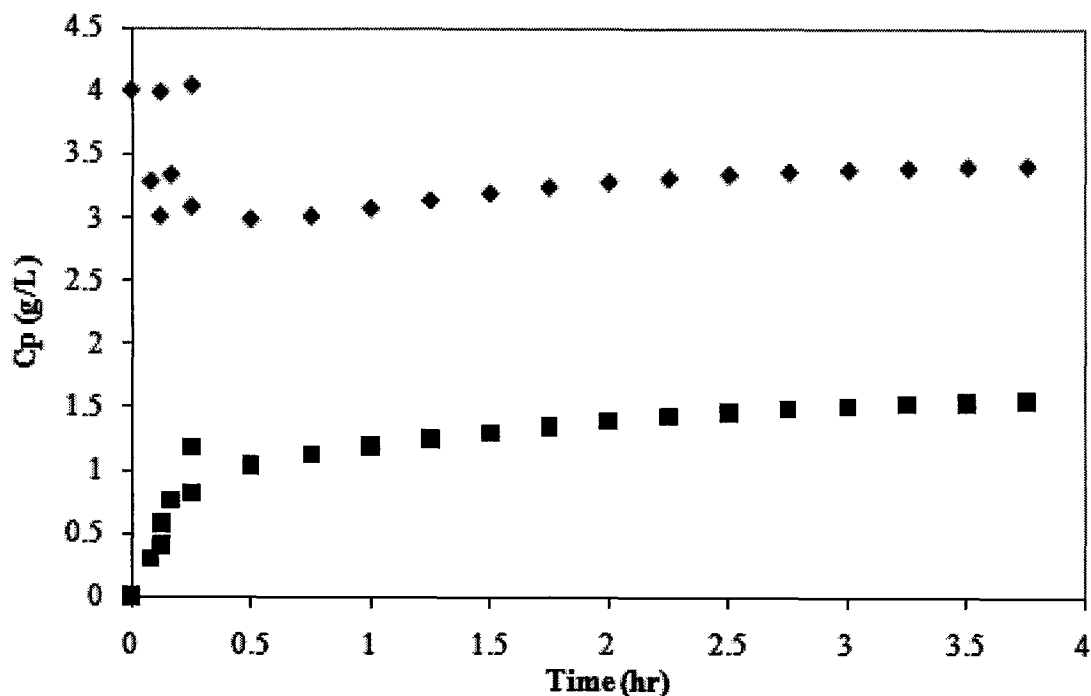


Figure 4.23 Concentration profile for three IV boluses with infusion of 0.695 g of drug with a loading dose of 0.82 g. The first and second maintenance doses are 0.201 g and 0.196 g respectively. The infusion rate was $R = 0.996 \text{ g/hr}$. The kinetic rate constants are $k_{12} = 1.0968 \text{ hr}^{-1}$, $k_{21} = 2.3596 \text{ hr}^{-1}$ and $k_{el} = 1.4335 \text{ hr}^{-1}$. The symbols (◆) and (■) represent the profile for the central and peripheral compartment respectively.

The drug administration regime developed to maintain 0.695 g of drug in the central compartment reaches equilibrium at 6.75 hours with IV infusion which is a very long time. The equilibrium is reached in 3.5 hours, when three IV boluses with infusion are administered. Thus, this is a better means of drug administration as compared to infusion if the plasma concentrations need to reach equilibrium as quickly as possible.

CHAPTER 5

CONCLUSION

The goal of the activities described herein was, to develop drug administration protocols based on well-stirred vessel experiments. The projects were setup in such a fashion as to mimic one- and two-compartment pharmacokinetic models. A one-compartment model assumes that the body is a single chamber. When an API is introduced into the body, the drug will be evenly distributed throughout the body. The experiments were conducted for IV bolus, multiple IV boluses, infusion and combined IV boluses with infusion. The kinetic parameters were calculated by using IV bolus data. These parameters were then used to design drug administration strategies for the investigated drug regimens. The results obtained from the experiments are in good agreement to those obtained from mathematical modeling.

The body can be broadly said to be divided into blood and tissues. This compartmentalization of the body then leads to the necessity of studying the distribution of the API between two regions or compartments. A two-compartment model assumes that the drug is distributed between the blood and tissue, and that the drug concentrations in both chambers, exhibit distinct transient behaviors. Stirred-vessels experiments were conducted to represent two-compartment models. The volume of each vessel was maintained at 200 mL in both the vessels. Administration protocols, similar to the ones in one-compartment model were used. Predicted and Experimental data were in good agreement.

5.1 Future Work

This study focuses on one- and two- compartment representation of the human body. The addition of more vessels may be more representative of physiologically-based pharmacokinetic (PBPK) models. The experiments performed used KMnO₄. The introduction of actual drug in the vessels should be studied. Experiments that incorporate absorption, metabolism and dissolution, would provide additional information to clinicians.

APPENDIX A
MASS BALANCE EQUATIONS FOR EXPERIMENTAL SETUP OF TWO
COMPARTMENT MODEL

The mass balance equations are derived from the experimental setup shown in Figure 2.6.

The mass balance around the central compartment in Figure 2.5 yields,

$$\frac{dm_1}{dt} = m_{I,1} - m_{el} - m_{12} + m_{21} \quad (\text{A.1})$$

and the mass balance over peripheral compartment in Figure 2.5 gives,

$$\frac{dm_2}{dt} = m_{I,2} + m_{12} - m_{21} \quad (\text{A.2})$$

where $m_{I,1}$ and $m_{I,2}$ are the rates of mass being added by the water inlet in the central and peripheral compartments respectively. Also m_{12} , m_{21} and m_{el} are the rates of mass being transferred from the central to the peripheral compartment, the mass being transferred from the peripheral to the central compartment and the mass being eliminated, respectively. The total mass in the system is not zero.

The change in volume in both the compartments can be obtained by dividing (A.1) and (A.2) with density.

$$\frac{dV_1}{dt} = F_{I,1} - F_{el} - F_{12} + F_{21} \quad (\text{A.3})$$

and

$$\frac{dV_2}{dt} = F_{I,2} + F_{12} - F_{21} \quad (\text{A.4})$$

where

V_1 is the volume of the central compartment,

V_2 is the volume of the peripheral compartment,

$F_{I,1}$ is the volumetric flow rate of water into the central compartment,

$F_{I,2}$ is the volumetric flow rate of water into the peripheral compartment,

F_{12} is the volumetric flow rate of water from the central to the peripheral compartment,

F_{21} is the volumetric flow rate of water from the peripheral to the central compartment,

and F_{el} is the volumetric flow rate of water being taken out from the central compartment.

As the volume in both the compartment is constant (A.3) and (A.4) become,

$$0 = F_{I,1} - F_{el} - F_{12} + F_{21} \quad (\text{A.5})$$

and

$$0 = F_{I,2} + F_{12} - F_{21} \quad (\text{A.6})$$

The mass balance for both the compartment yields

$$\frac{d(C_1 V_1)}{dt} = F_{I,1} C_{I,1} - F_{el} C_{el} - F_{12} C_1 + F_{21} C_2 \quad (\text{A.7})$$

and

$$\frac{d(C_2 V_2)}{dt} = F_{I,2} C_{I,2} + F_{12} C_1 - F_{21} C_2 \quad (\text{A.8})$$

Where C_1 , C_2 , $C_{I,1}$ and $C_{I,2}$ respectively stand for the concentration of the drug in the central compartment, the peripheral compartment, also $C_{I,1} = 0$ and $C_{I,2} = 0$. Also the

volumes in both the compartment are equal. The above equations (A.7) and (A.8) become,

$$\frac{dC_1}{dt} = -\frac{F_{el}C_{el}}{V_1} - \frac{F_{12}C_1}{V_1} + \frac{F_{21}C_2}{V_2} \quad (\text{A.9})$$

and

$$\frac{dC_2}{dt} = \frac{F_{12}C_1}{V_2} - \frac{F_{21}C_2}{V_2} \quad (\text{A.10})$$

From (A.9) and (A.10), it can be said that

$$k_{el} = \frac{F_{el}}{V_1} \quad (\text{A.11})$$

$$k_{21} = \frac{F_{21}}{V_1} = \frac{F_{21}}{V_2} \quad (\text{A.12})$$

$$k_{12} = \frac{F_{12}}{V_1} = \frac{F_{12}}{V_2} \quad (\text{A.13})$$

Thus (A.7) and (A.8) can be written as

$$\frac{dC_1}{dt} = -k_{el}C_{el} - k_{12}C_1 + k_{21}C_2 \quad (\text{A.14})$$

and

$$\frac{dC_2}{dt} = k_{12}C_1 - k_{21}C_2 \quad (\text{A.15})$$

APPENDIX B

LAPLACE TRANSFORM METHOD

This appendix shows on how to solve a differential equation using Laplace Transform. Assuming that the Laplace transforms of the dependent variable exists, the usual procedure to solve PDE is

1. Transform the PDE to an ordinary differential equation.
2. Transform the accompanying boundary conditions to those suitable for use with the ordinary differential equation.
3. Solve the resulting problem using known techniques, in this case variable separable method.
4. Invert the results to recover the solution to the PDE.

The inversion step can be relatively easy if the terms of step 3 can be located in a table of Laplace transforms. Without such a convenient table a more difficult technique involving the residue theorem has to be employed [19].

If $f(x)$ is a function, let $f(x)$ be defined for $0 < x < \infty$ and let s denote an arbitrary real variable. The Laplace transform of $f(x)$ is then defined as

$$L\{f(x)\} = F(s) = \int_0^{\infty} e^{-sx} f(x) dx$$

Now the inverse Laplace transform of $F(s)$ is defined $L^{-1}\{F(s)\}$, is another function $f(x)$ having the property that $L\{f(x)\} = F(s)$. The simplest technique for identifying inverse Laplace transforms is to read them from a table. If $F(s)$ is not in a recognizable form, it can be transformed into partial fractions.

An example of using Laplace transform from [20] is shown below:

$$y' - 5y = e^{7x}, y(0) = 0$$

Taking the Laplace transform of both sides of this differential equation yields

$$L\{y'\} - L\{5y\} = L\{e^{7x}\}$$

Using known properties of Laplace transforms the above equation becomes:

$$[sY(s) - 0] - 5Y(s) = \frac{1}{s-7}$$

From which it can be said that

$$Y(s) = \frac{1}{(s-5)(s-7)}$$

To the linear factors $s - 5$ and $s - 7$, the fractions $A/(s - 5)$ and $B/(s - 7)$ can be associated respectively.

$$\frac{1}{(s-5)(s-7)} = \frac{A}{s-5} + \frac{B}{s-7}$$

As a result,

$$1 = A(s-7) + B(s-5)$$

Substituting $s = 5$ and $s = 7$ we get $A = -1/2$ and $B = 1/2$.

So,

$$Y(s) = -\frac{1}{2(s-5)} + \frac{1}{2(s-7)}$$

Taking the inverse Laplace transform of $Y(s)$ gives,

$$L^{-1}\{Y(s)\} = L^{-1}\left\{-\frac{1}{2(s-5)}\right\} + L^{-1}\left\{\frac{1}{2(s-7)}\right\} = -\frac{e^{5x}}{2} + \frac{e^{7x}}{2}$$

All of the derivations in the text have been evaluated accordingly.

APPENDIX C

DATA ANALYSIS

C.1 Data analysis of One-Compartment Model

The data analysis is performed so as to calculate the value of the elimination rate constant. The concentration profile of a one-compartment model is represented by an exponential decay which is:

$$C_p(t) = A * e^{-\alpha * t} \quad (\text{A.16})$$

which can further be simplified to,

$$\ln(C_p(t)) = \ln(A) - \alpha * t \quad (\text{A.17})$$

A plot of $\ln(C_p)$ vs. t will now produce a straight line, which yields a slope of $-\alpha$ and an intercept of $\ln(A)$.

C.2 Data analysis of Two-Compartment Model

The data analysis is carried out to calculate the kinetic rate constants from the experiment. The concentration profile obtained is represented by a bi-exponential curve, which is:

$$C_p(t) = A * e^{-\alpha * t} + B * e^{-\beta * t} \quad (\text{A.18})$$

Since the first exponential term decays faster than the second exponential term, we can conclude that $\alpha \gg \beta$.

Hence, for large times:

$$C_p(t) = B * e^{-\beta * t} \quad (\text{A.19})$$

which can be written as,

$$\ln(Cp(t)) = \ln(B) - \beta * t \quad (\text{A.20})$$

A plot of $\ln(C_p)$ vs. t will now produce a straight line for larger times. This straight line will yield a slope of $-\beta$ and an intercept of $\ln(B)$.

Now since β and B are known, the equation (A.3) transforms into:

$$Cp(t) - B * e^{-\beta * t} = A * e^{-\alpha * t} \quad (\text{A.21})$$

and this can be simplified to be written as,

$$\ln(Cp(t) - B e^{-\beta * t}) = \ln(A) - \alpha * t \quad (\text{A.22})$$

A plot of $\ln(C_p)$ vs. t will now produce a straight line for smaller times. This straight line will yield a slope $-\alpha$ and an intercept of $\ln(A)$.

Now from the derivation of one IV bolus, as shown in Equation (2.27) we have:

$$A = \frac{C_{10}(\alpha - k_{21})}{(\alpha - \beta)} \quad (\text{A.23})$$

and

$$B = \frac{C_{10}(k_{21} - \beta)}{(\alpha - \beta)} \quad (\text{A.24})$$

Now dividing (A.23) by (A.24) gives,

$$\frac{A}{B} = \frac{\alpha - k_{21}}{k_{21} - \beta} \quad (\text{A.25})$$

Hence

$$k_{21} = \frac{A\beta + B\alpha}{A + B} \quad (\text{A.26})$$

It is also know from the derivation of one IV bolus that α and β are given by,

$$\alpha = \frac{-(k_{12} + k_{21} + k_{ei}) + \sqrt{(k_{12} + k_{21} + k_{ei})^2 - 4k_{ei}k_{21}}}{2}$$

$$\beta = \frac{-(k_{12} + k_{21} + k_{ei}) - \sqrt{(k_{12} + k_{21} + k_{ei})^2 - 4k_{ei}k_{21}}}{2}$$

here α refers to a and β refers to b from the derivation of one IV bolus.

Multiplying α and β gives,

$$k_{el} = \frac{\alpha\beta}{k_{21}} \quad (\text{A.27})$$

now adding α and β gives,

$$k_{12} = \alpha + \beta - k_{21} - k_{el} \quad (\text{A.28})$$

Hence the values of k_{12} , k_{21} and k_{el} can be calculated.

APPENDIX D

MATHEMATICA CODE

D.1 Mathematica Code for Optimization of Multiple IV boluses

The code shown below is used to optimize a multiple IV bolus regime, for the experiment performed. Contributed by Dr. Laurent Simon.

```

ClearAll["Global`*"];
Remove["Global`*"];
Off[General::"spell"]
Off[General::"spell1"]

k1 =0.0141; k2 = 0.01; ke =0.0155;

PENALTY=10;
twidth=0.5;
v1 = 7.811;
v2 = 9.502;
t1s=60;
y1t1s=4.5;
t2s=120;
y1t2s=4.5;
t3s = 200;
y1t3s = 4.5;
tf = 300;
ylinis = 4.5;
y1sets = (0.2) v2;

sol1[ylini_?NumericQ, t1_?NumericQ, t2_?NumericQ,
y1t1_?NumericQ, y1t2_?NumericQ]:=
{y1[t], y2[t]}/.
NDSolve[{y1'[t]==- k1 y1[t] + k2 y2[t] - ke y1[t] + PENALTY (y1t1-y1[t])Exp[-((t-
t1)/twidth)^2]+PENALTY (y1t2-y1[t])Exp[-((t-t2)/twidth)^2] ,y2'[t]== k1 y1[t]- k2 y2[t], y1[0]==ylini,
y2[0]==0.0},{y1, y2},{t,0.0,tf}][[1]];

```

```

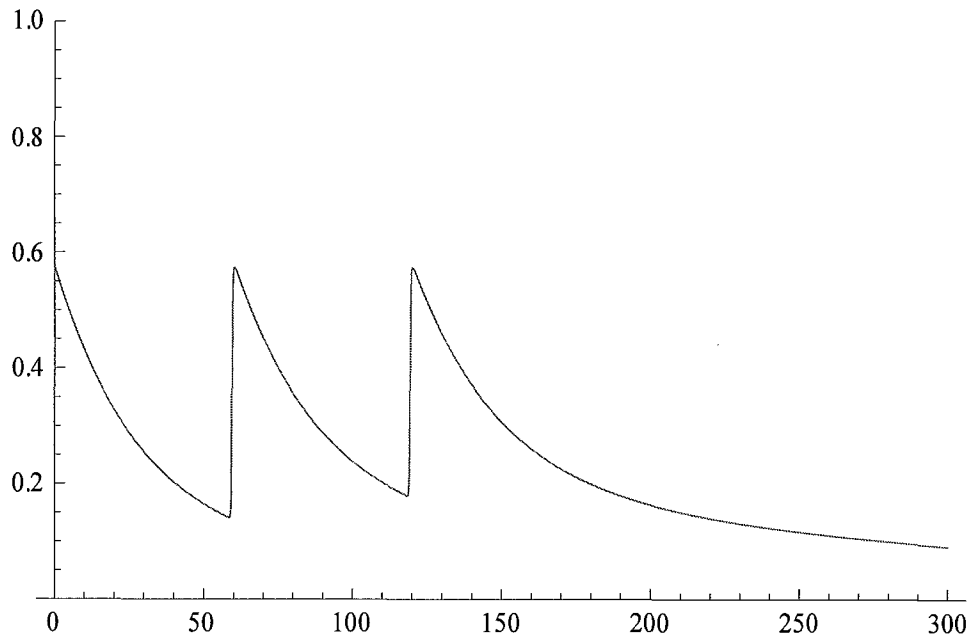
Y1[ylini_, t1_, t2_, y1t1_, y1t2_, te_] := sol1[ylini, t1,
t2, y1t1, y1t2][[1]] /. t -> te;
Y2[ylini_, t1_, t2_, y1t1_, y1t2_, te_] := sol1[ylini, t1,
t2, y1t1, y1t2][[2]] /. t -> te;

```

```

Plot[1/v1 Y1[ylinis, t1s, t2s, y1t1s, y1t2s, t1],
{t1, 0, tf}, PlotRange -> {0, 1}]

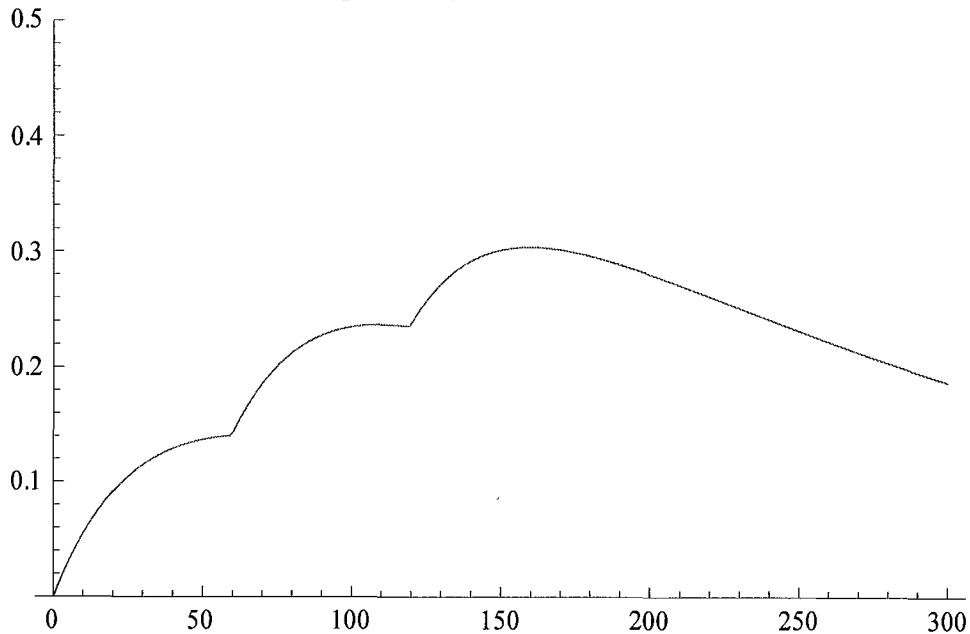
```



```

Plot[1/v2 Y2[ylinis, t1s, t2s, y1t1s, y1t2s, t1],
{t1, 0, tf}, PlotRange -> {0, 0.5}]

```

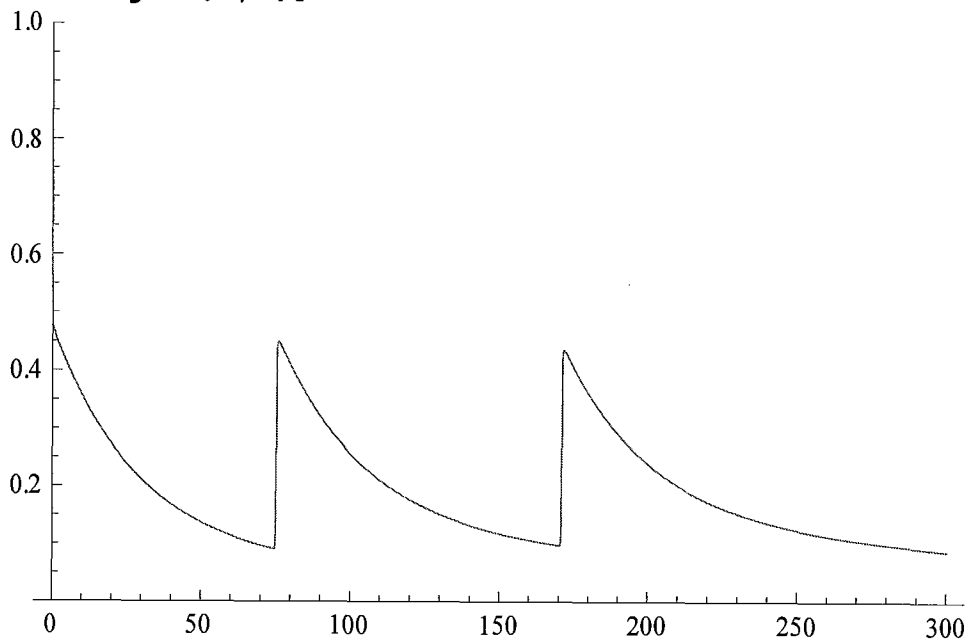


```
error[ylini_?NumericQ, t1_?NumericQ, t2_?NumericQ,
y1t1_?NumericQ, y1t2_?NumericQ]:=NIntegrate[(y1sets-
sol1[ylini, t1, t2, y1t1, y1t2][[1]])^2, {t,0,tf}]
```

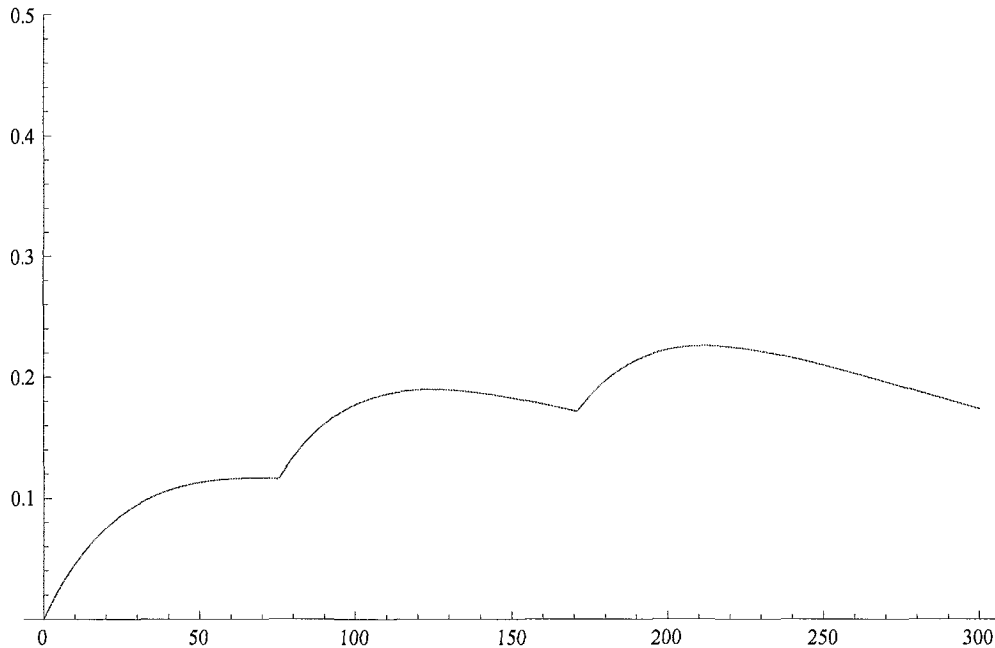
```
var={ylini, t1, t2, y1t1, y1t2}
{ylini,t1,t2,y1t1,y1t2}
```

```
Table[NMinimize[{error[ylini, t1, t2, y1t1, y1t2],10^-
10<ylini<10, 10^-10<t2<tf,10^-10<y1t1<10,10^-10< y1t2<10, t1 <
t2},var,
StepMonitor:>Print[{ylini,t1,t2,y1t1,y1t2,error[ylini, t1,
t2,y1t1, y1t2] }],MaxIterations->500] ,{i,1}]]//Timing
```

```
Plot[Evaluate[1/v1
Y1[3.7216665062542953`,75.81998939050332`,171.5934461872726
`,3.526467545530771`,3.416639971477414`, t] ], {t,0,tf},
PlotRange->{0,1}]
```



```
Plot[Evaluate[1/v2
Y2[3.7216665062542953`,75.81998939050332`,171.5934461872726
`,3.526467545530771`,3.416639971477414`, t] ], {t,0,tf},
PlotRange->{0,0.5}]
```



D.2 Mathematica Code for Optimization of IV boluses with Infusion

The code shown below is used to optimize a multiple IV bolus with infusion regime, for the experiment performed. Contributed by Kwang Seok Kim.

```
Quit[]
k1=2.73(*h^-1*);k2=3.11(*h^-1*);ke=.312(*h^-
1*);yset=193.9(*mg*);tf=3(*h*);NB=6;

$$\delta = \sqrt{4 k_2 k_e \left[ \frac{k_1}{k_1 + k_2 + k_e} \right]^2}$$
;  $\alpha = k_1 + k_2 + k_e + \delta$ ;  $\beta = k_1 + k_2 + k_e -$ 
 $\delta$ ;  $\gamma = k_1 - k_2 + k_e - \delta$ ;  $\epsilon = k_1 + k_2 - k_e + \delta$ ;  $\phi = k_1 - k_2 + k_e + \delta$ ;  $\eta = k_1 + k_2 - k_e - \delta$ ;
y1[0][0]=0;y2[0][0]=0;Table[Ri[j]=0,{j,NB-1}];
Ri[NB]=ke yset;
objfn[tm_,Mb_,NB_] := Module[{y1,y2,Ri,err},
  Table[Ri[j]=0,{j,NB-1}];
  Ri[NB]=ke yset;
  y1[0][0]=0;y2[0][0]=0;
  y1[j_][t_] := Ri[j]/ke - 1/(2  $\delta$ ) ( $\gamma$  (y1[j-
1][tm[[j]]]+Mb[[j]]) - 2 k2 y2[j-1][tm[[j]]] +  $\epsilon$  Ri[j]/ke)
```

```

~  $\frac{1}{2} \sqrt{\frac{1}{\delta^2} \left( \phi(y1[j-1][tm[[j]]]+Mb[[j]])-2 k2 y2[j-1][tm[[j]]]+Ri[j] /ke \eta) \right)}$ 
+1/(2δ) (φ (y1[j-1][tm[[j]]]+Mb[[j]])-2 k2
~  $\frac{1}{2} \sqrt{\frac{1}{\delta^2} \left( \phi(y1[j-1][tm[[j]]]+Mb[[j]])-2 k2 y2[j-1][tm[[j]]]+Ri[j] /ke \eta) \right)}$ 
y2[j-1][tm[[j]]]+Ri[j] /ke η) ;
y2[j_][t_]:= (k1 Ri[j])/(k2 ke)-1/(4k2 δ) φ ( γ (y1[j-
1][tm[[j]]]+Mb[[j]])- 2 k2 y2[j-1][tm[[j]]]+ε Ri[j]/ke)
~  $\frac{1}{2} \sqrt{\frac{1}{\delta^2} \left( \phi(y1[j-1][tm[[j]]]+Mb[[j]])-2 k2 y2[j-1][tm[[j]]]+Ri[j] /ke \eta) \right)}$ 
+1/(4k2 δ) γ (φ (y1[j-1][tm[[j]]]+Mb[[j]])-2
~  $\frac{1}{2} \sqrt{\frac{1}{\delta^2} \left( \phi(y1[j-1][tm[[j]]]+Mb[[j]])-2 k2 y2[j-1][tm[[j]]]+Ri[j] /ke \eta) \right)}$ 
k2 y2[j-1][tm[[j]]]+Ri[j] /ke η) ;

err[j_]:= (tm[[j+1]]-tm[[j]]) (Ri[j]/ke-yset)2+1/(4δ2 α)
(φ (y1[j-1][tm[[j]]]+Mb[[j]])-2 k2 y2[j-1][tm[[j]]]+Ri[j]
/ke η)2 (1-⊙-(tm[[j+1]]-tm[[j]]) α)+1/(δ α) 2 (φ (y1[j-
1][tm[[j]]]+Mb[[j]])-2 k2 y2[j-1][tm[[j]]]+Ri[j] /ke
~  $\frac{1}{2} \sqrt{\frac{1}{\delta^2} \left( \phi(y1[j-1][tm[[j]]]+Mb[[j]])-2 k2 y2[j-1][tm[[j]]]+Ri[j] /ke \eta) \right)}$ 
η) (Ri[j]/ke-yset) (1-~  $\frac{1}{2} \sqrt{\frac{1}{\delta^2} \left( \phi(y1[j-1][tm[[j]]]+Mb[[j]])-2 k2 y2[j-1][tm[[j]]]+Ri[j] /ke \eta) \right)}$ 
)-2/(δ β) (γ
(y1[j-1][tm[[j]]]+Mb[[j]])- 2 k2 y2[j-1][tm[[j]]]+ε
~  $\frac{1}{2} \sqrt{\frac{1}{\delta^2} \left( \phi(y1[j-1][tm[[j]]]+Mb[[j]])-2 k2 y2[j-1][tm[[j]]]+Ri[j] /ke \eta) \right)}$ 
Ri[j]/ke) (1-~  $\frac{1}{2} \sqrt{\frac{1}{\delta^2} \left( \phi(y1[j-1][tm[[j]]]+Mb[[j]])-2 k2 y2[j-1][tm[[j]]]+Ri[j] /ke \eta) \right)}$ 
) (Ri[j]/ke-yset)+1/(4
δ2 β) (γ (y1[j-1][tm[[j]]]+Mb[[j]])- 2 k2 y2[j-1][tm[[j]]]+ε
Ri[j]/ke)2 (1-⊙-(tm[[j+1]]-tm[[j]]) β)-1/((α+β) δ2) (γ (y1[j-
1][tm[[j]]]+Mb[[j]])- 2 k2 y2[j-1][tm[[j]]]+ε Ri[j]/ke) (φ
(y1[j-1][tm[[j]]]+Mb[[j]])-2 k2 y2[j-1][tm[[j]]]+Ri[j] /ke
~  $\frac{1}{2} \sqrt{\frac{1}{\delta^2} \left( \phi(y1[j-1][tm[[j]]]+Mb[[j]])-2 k2 y2[j-1][tm[[j]]]+Ri[j] /ke \eta) \right)}$ 
η) (1-~  $\frac{1}{2} \sqrt{\frac{1}{\delta^2} \left( \phi(y1[j-1][tm[[j]]]+Mb[[j]])-2 k2 y2[j-1][tm[[j]]]+Ri[j] /ke \eta) \right)}$ 
);

```

```

obj=  $\sqrt{\text{TotalTable err[j], j, NB}} / (tm[[NB+1]]$ 
yset)
];

```

```

ToExpression[StringJoin["fabcd",Table[{"arg",ToString[i],"_
?NumericQ,"},{i,2,2NB-
1}],{"arg",ToString[2NB],"_?NumericQ]:=objfn[{0,"},Table[{"
arg",ToString[i],"},{i,2,NB}],ToString[tf],"},{Table[{"
arg",ToString[i],"},{i,NB+1,2NB-
1}],{"arg",ToString[2NB],"},ToString[NB],""]}]

```

```

opt=ToExpression[StringJoin["NMinimize[{rr=fabcd",Table[{"a
rg",ToString[i],"},{i,2,2NB-

```

```

1}},{ "arg",ToString[2NB]}},",",0",Table[{"<arg",ToString[i]},
{i,2,NB}], "<tf",Table[{"",0<arg",ToString[i]}, {i,NB+1,2NB}],
"}, {"",Table[{"{arg",ToString[i],",",ToString[.5tf (i-
1)/NB],",",ToString[1.05*.5tf (i-
1)/NB],",",{"{i,2,NB}],Table[{"{arg",ToString[i],",",ToStri
ng[(1.1*yset)/(i-NB)],",",ToString[1.1 (1.1*yset)/(i-
NB)],",",{"{i,NB+1,2NB-
1}},{ "{arg",ToString[2NB],",",ToString[(1.1*yset)/NB],",",T
oString[1.1 (1.1*yset)/NB],"}"}}, {"",Method-
>NelderMead,StepMonitor:>Print[{"",Table[{"arg",ToString[i],
",",{"{i,2,2NB}],"rr}]]//Timing"]}

```

```

{0.256844,0.524692,0.763214,1.02454,1.27777,218.152,108.788
,77.0006,54.386,45.6221,35.8972,0.120199}

```

```

{0.261794,0.507003,0.739698,1.07134,1.28919,228.126,102.492
,69.5479,53.0547,40.7593,36.285,0.106997}

```

```

{0.261794,0.507003,0.739698,1.07134,1.28919,228.126,102.492
,69.5479,53.0547,40.7593,36.285,0.106997}

```

```

{0.261794,0.507003,0.739698,1.07134,1.28919,228.126,102.492
,69.5479,53.0547,40.7593,36.285,0.106997}

```

```

{0.261794,0.507003,0.739698,1.07134,1.28919,228.126,102.492
,69.5479,53.0547,40.7593,36.285,0.106997}

```

```

{0.261794,0.507003,0.739698,1.07134,1.28919,228.126,102.492
,69.5479,53.0547,40.7593,36.285,0.106997}

```

```

{0.265709,0.524691,0.77833,1.091,1.28374,203.585,103.276,70
.7459,53.709,48.2389,34.1232,0.0981872}

```

```

{0.265709,0.524691,0.77833,1.091,1.28374,203.585,103.276,70
.7459,53.709,48.2389,34.1232,0.0981872}

```

```

{0.265709,0.524691,0.77833,1.091,1.28374,203.585,103.276,70
.7459,53.709,48.2389,34.1232,0.0981872}

```

```

{0.261292,0.524978,0.768091,1.09177,1.31972,205.786,105.723
,63.2749,49.3023,45.6322,35.1527,0.0859107}

```

```

{0.261292,0.524978,0.768091,1.09177,1.31972,205.786,105.723
,63.2749,49.3023,45.6322,35.1527,0.0859107}

```

```

{0.261292,0.524978,0.768091,1.09177,1.31972,205.786,105.723
,63.2749,49.3023,45.6322,35.1527,0.0859107}

```


{0.260851,0.497845,0.758532,1.13847,1.33182,195.021,104.448
,57.2816,47.8493,43.9384,35.3271,0.0728156}

{0.260851,0.497845,0.758532,1.13847,1.33182,195.021,104.448
,57.2816,47.8493,43.9384,35.3271,0.0728156}

{0.260851,0.497845,0.758532,1.13847,1.33182,195.021,104.448
,57.2816,47.8493,43.9384,35.3271,0.0728156}

{0.260851,0.497845,0.758532,1.13847,1.33182,195.021,104.448
,57.2816,47.8493,43.9384,35.3271,0.0728156}

{0.260851,0.497845,0.758532,1.13847,1.33182,195.021,104.448
,57.2816,47.8493,43.9384,35.3271,0.0728156}

{0.260851,0.497845,0.758532,1.13847,1.33182,195.021,104.448
,57.2816,47.8493,43.9384,35.3271,0.0728156}

{0.266224,0.5312,0.778558,1.19951,1.36635,194.246,90.5743,5
1.6953,39.162,47.1681,34.4037,0.0667614}

{0.266224,0.5312,0.778558,1.19951,1.36635,194.246,90.5743,5
1.6953,39.162,47.1681,34.4037,0.0667614}

{0.262797,0.511979,0.73595,1.15584,1.33733,194.601,96.0628,
53.8296,42.4777,42.0683,33.6936,0.06357}

{0.262797,0.511979,0.73595,1.15584,1.33733,194.601,96.0628,
53.8296,42.4777,42.0683,33.6936,0.06357}

{0.262797,0.511979,0.73595,1.15584,1.33733,194.601,96.0628,
53.8296,42.4777,42.0683,33.6936,0.06357}

{0.262797,0.511979,0.73595,1.15584,1.33733,194.601,96.0628,
53.8296,42.4777,42.0683,33.6936,0.06357}

{0.262797,0.511979,0.73595,1.15584,1.33733,194.601,96.0628,
53.8296,42.4777,42.0683,33.6936,0.06357}

{0.262797,0.511979,0.73595,1.15584,1.33733,194.601,96.0628,
53.8296,42.4777,42.0683,33.6936,0.06357}

{0.276033,0.499443,0.713619,1.28151,1.3681,219.943,77.9381,
39.3218,39.138,35.8432,34.0357,0.0549382}

{0.276033,0.499443,0.713619,1.28151,1.3681,219.943,77.9381,

39.3218,39.138,35.8432,34.0357,0.0549382}

{0.276033,0.499443,0.713619,1.28151,1.3681,219.943,77.9381,
39.3218,39.138,35.8432,34.0357,0.0549382}

{0.276033,0.499443,0.713619,1.28151,1.3681,219.943,77.9381,
39.3218,39.138,35.8432,34.0357,0.0549382}

{0.276033,0.499443,0.713619,1.28151,1.3681,219.943,77.9381,
39.3218,39.138,35.8432,34.0357,0.0549382}

{0.276033,0.499443,0.713619,1.28151,1.3681,219.943,77.9381,
39.3218,39.138,35.8432,34.0357,0.0549382}

{0.276033,0.499443,0.713619,1.28151,1.3681,219.943,77.9381,
39.3218,39.138,35.8432,34.0357,0.0549382}

{0.276033,0.499443,0.713619,1.28151,1.3681,219.943,77.9381,
39.3218,39.138,35.8432,34.0357,0.0549382}

{0.276033,0.499443,0.713619,1.28151,1.3681,219.943,77.9381,
39.3218,39.138,35.8432,34.0357,0.0549382}

{0.276033,0.499443,0.713619,1.28151,1.3681,219.943,77.9381,
39.3218,39.138,35.8432,34.0357,0.0549382}

{0.276033,0.499443,0.713619,1.28151,1.3681,219.943,77.9381,
39.3218,39.138,35.8432,34.0357,0.0549382}

{0.250764,0.526959,0.75088,1.24455,1.41681,237.615,79.5691,
33.1756,34.8772,33.7503,40.0537,0.0468644}

{0.250764,0.526959,0.75088,1.24455,1.41681,237.615,79.5691,
33.1756,34.8772,33.7503,40.0537,0.0468644}

{0.250764,0.526959,0.75088,1.24455,1.41681,237.615,79.5691,
33.1756,34.8772,33.7503,40.0537,0.0468644}

{0.250764,0.526959,0.75088,1.24455,1.41681,237.615,79.5691,
33.1756,34.8772,33.7503,40.0537,0.0468644}

{0.250764,0.526959,0.75088,1.24455,1.41681,237.615,79.5691,
33.1756,34.8772,33.7503,40.0537,0.0468644}

{0.263707,0.500701,0.721715,1.28121,1.42126,245.623,78.6553,
34.5749,35.2995,33.6475,38.4834,0.046347}

{0.263707,0.500701,0.721715,1.28121,1.42126,245.623,78.6553
,34.5749,35.2995,33.6475,38.4834,0.046347}

{0.263707,0.500701,0.721715,1.28121,1.42126,245.623,78.6553
,34.5749,35.2995,33.6475,38.4834,0.046347}

{0.263707,0.500701,0.721715,1.28121,1.42126,245.623,78.6553
,34.5749,35.2995,33.6475,38.4834,0.046347}

{0.263707,0.500701,0.721715,1.28121,1.42126,245.623,78.6553
,34.5749,35.2995,33.6475,38.4834,0.046347}

{0.26258,0.506101,0.700213,1.26567,1.39091,251.932,74.7098,
37.1607,36.3779,30.5029,37.7239,0.0458202}

{0.257581,0.50856,0.706508,1.28737,1.39827,257.171,72.5289,
34.8305,35.6718,28.7054,38.2607,0.045108}

{0.262767,0.499935,0.703367,1.30487,1.44121,260.993,70.7219
,24.2106,31.5732,25.7524,40.5628,0.0445926}

{0.262767,0.499935,0.703367,1.30487,1.44121,260.993,70.7219
,24.2106,31.5732,25.7524,40.5628,0.0445926}

{0.262767,0.499935,0.703367,1.30487,1.44121,260.993,70.7219
,24.2106,31.5732,25.7524,40.5628,0.0445926}

{0.262767,0.499935,0.703367,1.30487,1.44121,260.993,70.7219
,24.2106,31.5732,25.7524,40.5628,0.0445926}

{0.262767,0.499935,0.703367,1.30487,1.44121,260.993,70.7219
,24.2106,31.5732,25.7524,40.5628,0.0445926}

{0.262767,0.499935,0.703367,1.30487,1.44121,260.993,70.7219
,24.2106,31.5732,25.7524,40.5628,0.0445926}

{0.262767,0.499935,0.703367,1.30487,1.44121,260.993,70.7219
,24.2106,31.5732,25.7524,40.5628,0.0445926}

{0.25778,0.505098,0.701505,1.30259,1.43124,256.834,71.2069,
27.6554,32.1395,27.7669,39.4803,0.044225}

{0.25778,0.505098,0.701505,1.30259,1.43124,256.834,71.2069,
27.6554,32.1395,27.7669,39.4803,0.044225}

{0.25778,0.505098,0.701505,1.30259,1.43124,256.834,71.2069,
27.6554,32.1395,27.7669,39.4803,0.044225}

{0.25778,0.505098,0.701505,1.30259,1.43124,256.834,71.2069,
27.6554,32.1395,27.7669,39.4803,0.044225}

{0.257014,0.501918,0.674611,1.28554,1.40903,267.47,66.9127,
29.2206,32.2282,22.807,39.4542,0.0426237}

{0.257014,0.501918,0.674611,1.28554,1.40903,267.47,66.9127,
29.2206,32.2282,22.807,39.4542,0.0426237}

{0.257014,0.501918,0.674611,1.28554,1.40903,267.47,66.9127,
29.2206,32.2282,22.807,39.4542,0.0426237}

{0.257014,0.501918,0.674611,1.28554,1.40903,267.47,66.9127,
29.2206,32.2282,22.807,39.4542,0.0426237}

{0.257014,0.501918,0.674611,1.28554,1.40903,267.47,66.9127,
29.2206,32.2282,22.807,39.4542,0.0426237}

{0.257014,0.501918,0.674611,1.28554,1.40903,267.47,66.9127,
29.2206,32.2282,22.807,39.4542,0.0426237}

{0.257014,0.501918,0.674611,1.28554,1.40903,267.47,66.9127,
29.2206,32.2282,22.807,39.4542,0.0426237}

{0.257014,0.501918,0.674611,1.28554,1.40903,267.47,66.9127,
29.2206,32.2282,22.807,39.4542,0.0426237}

{0.257014,0.501918,0.674611,1.28554,1.40903,267.47,66.9127,
29.2206,32.2282,22.807,39.4542,0.0426237}

{0.257014,0.501918,0.674611,1.28554,1.40903,267.47,66.9127,
29.2206,32.2282,22.807,39.4542,0.0426237}

{0.257014,0.501918,0.674611,1.28554,1.40903,267.47,66.9127,
29.2206,32.2282,22.807,39.4542,0.0426237}

{0.257014,0.501918,0.674611,1.28554,1.40903,267.47,66.9127,
29.2206,32.2282,22.807,39.4542,0.0426237}

{0.257014,0.501918,0.674611,1.28554,1.40903,267.47,66.9127,
29.2206,32.2282,22.807,39.4542,0.0426237}

{0.257014,0.501918,0.674611,1.28554,1.40903,267.47,66.9127,
29.2206,32.2282,22.807,39.4542,0.0426237}

{0.257436,0.49706,0.686692,1.27825,1.4373,258.46,73.4372,28

{0.257014,0.501918,0.674611,1.28554,1.40903,267.47,66.9127,
29.2206,32.2282,22.807,39.4542,0.0426237}

{0.257014,0.501918,0.674611,1.28554,1.40903,267.47,66.9127,
29.2206,32.2282,22.807,39.4542,0.0426237}

{0.257014,0.501918,0.674611,1.28554,1.40903,267.47,66.9127,
29.2206,32.2282,22.807,39.4542,0.0426237}

{0.257014,0.501918,0.674611,1.28554,1.40903,267.47,66.9127,
29.2206,32.2282,22.807,39.4542,0.0426237}

{0.257014,0.501918,0.674611,1.28554,1.40903,267.47,66.9127,
29.2206,32.2282,22.807,39.4542,0.0426237}

{0.257014,0.501918,0.674611,1.28554,1.40903,267.47,66.9127,
29.2206,32.2282,22.807,39.4542,0.0426237}

{0.257014,0.501918,0.674611,1.28554,1.40903,267.47,66.9127,
29.2206,32.2282,22.807,39.4542,0.0426237}

{0.257014,0.501918,0.674611,1.28554,1.40903,267.47,66.9127,
29.2206,32.2282,22.807,39.4542,0.0426237}

{0.257014,0.501918,0.674611,1.28554,1.40903,267.47,66.9127,
29.2206,32.2282,22.807,39.4542,0.0426237}

{0.257014,0.501918,0.674611,1.28554,1.40903,267.47,66.9127,
29.2206,32.2282,22.807,39.4542,0.0426237}

{0.257014,0.501918,0.674611,1.28554,1.40903,267.47,66.9127,
29.2206,32.2282,22.807,39.4542,0.0426237}

{0.257436,0.49706,0.686692,1.27825,1.4373,258.46,73.4372,28
.5185,30.6021,26.2144,40.0467,0.0425364}

{0.257436,0.49706,0.686692,1.27825,1.4373,258.46,73.4372,28
.5185,30.6021,26.2144,40.0467,0.0425364}

{0.238897,0.513469,0.702622,1.23204,1.44689,256.337,78.7969
,28.2836,29.0184,25.148,42.2688,0.041524}

{0.238897,0.513469,0.702622,1.23204,1.44689,256.337,78.7969
,28.2836,29.0184,25.148,42.2688,0.041524}

{0.237695,0.518804,0.671366,1.19032,1.3894,251.715,77.1318,
38.252,31.4594,24.3302,38.9951,0.0401419}

{0.229687,0.524609,0.670116,1.18195,1.41796,253.15,76.4631,
30.727,27.9083,21.4219,41.2665,0.0398154}

{0.23429,0.517425,0.684092,1.18096,1.41416,247.148,79.32,34
.9535,29.0971,24.6074,40.9644,0.0396665}

{0.23429,0.517425,0.684092,1.18096,1.41416,247.148,79.32,34
.9535,29.0971,24.6074,40.9644,0.0396665}

{0.229731,0.512676,0.672652,1.18344,1.41609,250.143,81.1045
,36.4801,29.168,24.4768,40.6036,0.03962}

{0.229731,0.512676,0.672652,1.18344,1.41609,250.143,81.1045
,36.4801,29.168,24.4768,40.6036,0.03962}

{0.23297,0.511146,0.617707,1.14587,1.36916,253.784,74.1137,
40.9961,29.2262,19.2592,38.1889,0.0378068}

{0.23297,0.511146,0.617707,1.14587,1.36916,253.784,74.1137,
40.9961,29.2262,19.2592,38.1889,0.0378068}

{0.23297,0.511146,0.617707,1.14587,1.36916,253.784,74.1137,
40.9961,29.2262,19.2592,38.1889,0.0378068}

{0.23297,0.511146,0.617707,1.14587,1.36916,253.784,74.1137,
40.9961,29.2262,19.2592,38.1889,0.0378068}

{0.23297,0.511146,0.617707,1.14587,1.36916,253.784,74.1137,
40.9961,29.2262,19.2592,38.1889,0.0378068}

{0.356444,0.822577,1.34913,2.31252,2.98369,287.075,94.9242,
59.6628,44.5176,30.462,45.799,0.0579231}

{0.286683,0.743077,1.30586,2.19906,2.93302,270.144,92.9815,
60.4859,48.4838,35.8274,43.211,0.0523917}

{0.284202,0.729388,1.33023,2.13582,2.40913,270.142,92.9796,
60.4843,48.4825,35.8264,43.2095,0.058474}

{0.216459,0.542905,1.10056,1.94259,2.328,251.727,86.8389,61
.9098,47.7887,32.0263,25.4833,0.043126}

{0.181972,0.442113,0.845311,1.47267,2.15322,242.821,78.362,
61.005,47.2683,40.265,22.9433,0.0374787}

{0.14695,0.337169,0.582904,0.95779,1.44537,234.1,68.1373,55
.1694,42.6518,32.2488,19.2305,0.0277599}

{0.12011,0.26782,0.443346,0.646658,0.892883,226.954,58.8343
,49.2466,38.5945,27.2086,16.8746,0.0206291}

{0.0950424,0.208192,0.341205,0.491272,0.617853,220.676,48.3
938,42.8374,36.1295,28.1633,21.5521,0.0180815}

{0.0883859,0.193007,0.317365,0.465097,0.640889,219.102,45.0
136,40.5918,35.5697,30.2027,28.4051,0.0174272}

{0.0854971,0.186568,0.308535,0.459051,0.646583,218.609,43.3
022,39.6415,35.8832,32.3294,29.2504,0.0173876}

{0.,-5.16319,-3.71373,-
1.03061,3.,0.,0.,806.291,1007.94,1276.85,0.,2.8962}
{0.,-5.16319,-3.71373,-
1.03061,3.,0.,0.,806.291,1007.94,1276.85,0.,2.8962}
{0.,-5.16166,-3.71373,-
1.03061,3.,0.,0.,806.291,1007.94,1276.85,0.,2.89642}
{0.,-5.16166,-3.71373,-
1.03061,3.,0.,0.,806.291,1007.94,1276.85,0.,2.89642}
{0.,-5.13717,-3.71373,-
1.03061,3.,0.,0.,806.291,1007.94,1276.85,0.,2.90005}
{0.,-5.03014,-3.71373,-
1.03061,3.,0.,0.,806.291,1007.94,1276.85,0.,2.91601}
{0.,-4.38831,-3.71373,-
1.03061,3.,0.,0.,806.291,1007.94,1276.85,0.,3.01633}
{0.,-4.38831,-3.71373,-
1.03061,3.,0.,0.,806.291,1007.94,1276.85,0.,3.01633}
{0.,-3.37165,-3.71373,-
1.03061,3.,0.,0.,806.291,1007.94,1276.85,0.,3.52568}
{0.,-2.31765,-3.59472,-
1.03061,3.,0.,0.,806.291,1007.94,1276.85,0.,25.0378}

{0.241343,0.770011,1.88172,3.,3.,0.000344349,0.000347668,80
6.29,1007.93,1276.85,0.,1.34799}

{0.241343,0.770011,1.88172,3.,3.,0.000344349,0.000347668,80
6.29,1007.93,1276.85,0.,1.34799}

{1785.67,{0.0173875,{arg2→0.0853353,arg3→0.186165,arg4→0.3
07957,arg5→0.458314,arg6→0.64555,arg7→218.602,arg8→43.190
6,arg9→39.5977,arg10→35.9248,arg11→32.3445,arg12→29.2819}
}}

```
opt={1785.672`,{0.017387540465247445`,{arg2→0.0853353341333
4127`,arg3→0.18616538388712472`,arg4→0.30795732355473754`,
arg5→0.4583143854064272`,arg6→0.645550076680361`,arg7→218.
60226499366627`,arg8→43.19062768697064`,arg9→39.5976646980
12515`,arg10→35.9248352640499`,arg11→32.344509517611264`,a
rg12→29.281883338641578`}}}
```

```
{1785.67,{0.0173875,{arg2→0.0853353,arg3→0.186165,arg4→0.3
07957,arg5→0.458314,arg6→0.64555,arg7→218.602,arg8→43.190
6,arg9→39.5977,arg10→35.9248,arg11→32.3445,arg12→29.2819}
}}
```

```
NB=6;
```

```
tm=Flatten[{{0},Table[opt[[2,2,i,2]],{i,NB-
1}},{tf}]];Mb=Table[opt[[2,2,i,2]],{i,NB,2NB-1}];
```

```
60*tm
```

```
{0,5.12012,11.1699,18.4774,27.4989,38.733,60 tf}
```

```
Mb
```

```
{218.602,43.1906,39.5977,35.9248,32.3445,29.2819}
```


REFERENCES

- [1] Leon Shargel, Susanna Wu-Pong and Andrew B. C. Yu, "*Applied Biopharmaceutics and Pharmacokinetics*". Fifth edition.
- [2] Howard .C. Ansel, Loyd .V. Allen Jr. and Nicholas .G. Popovich, " *Pharmaceutical dosage forms and drug delivery systems*". Seventh edition.
- [3] Edited by Praveen Tyle, "*Drug delivery devices, fundamentals and application*". Volume 32.
- [4] Grazia Stagni, and Chinmay Shukla, "*Pharmacokinetics of methotrexate in rabbit skin and plasma after iv-bolus and iontophoretic administrations.*". Journal of Controlled Release, Volume 93, Issue 3, 12 December 2003, Pages 283-292.
- [5] Richard E. Sweeney, and Donald M. Maxwell, "*A theoretical expression for the protection associated with stoichiometric and catalytic scavengers in a single compartment model of organophosphorus poisoning*1*". Mathematical Biosciences, Volume 181, Issue 2, February 2003, Pages 133-143.
- [6] Schoenwald, R.D., "*Pharmacokinetic Principles of Dosing Adjustments*", CRC Press, Boca Raton, 2001.
- [7] Truskey, G.A., F. Yuan, and D.F. Katz, "*Transport Phenomena in Biological Systems*". Second Edition, Pearson Prentice Hall, Upper Saddle River, NJ, 2009.
- [8] Sanyi Tang and Yanni Xiao, "*One-compartment model with Michaelis-Menten elimination kinetics and therapeutic window: an analytical approach*". Journal of Pharmacokinetics and Pharmacodynamics, Volume 34, Issue 6, December 2007, Pages 807-827.
- [9] Saadeddin, A., F. Torres-Molina, J. Cárcel-Trullols, A. Araico, and J.E. Peris, "*Pharmacokinetics of the time-dependent elimination of all-trans-retinoic acid in rats,*" AAPS PharmSci, Volume 6, Issue 1, First Edition. 2004.
- [10] Larry A. Bauer, "*Clinical Pharmacokinetics Handbook*", McGraw-Hill.
- [11] R. Kaufmann, R. Bayer, T. Färniss, H. Krause and H. Tritthart, "*Calcium-movement controlling cardiac contractility. II. Analog computation of cardiac excitation-contraction coupling on the basis of calcium kinetics in a multi-compartment model*1, *2*". Journal of Molecular and Cellular Cardiology, Volume 6, Issue 6, December 1974, Pages 543-559.
- [12] Grazia Stagni , , Md Ehsan Ali and Daniella Weng, " *Pharmacokinetics of acyclovir in rabbit skin after IV-bolus, ointment, and iontophoretic administrations*".

International Journal of Pharmaceutics, Volume 274, Issues 1-2, 15 April 2004, Pages 201-211.

- [13] Pierre Yves Grosse, Françoise Bressolle, Philippe Rouanet, Jean Michel Joulia and Frédéric Pinguet, "*Methyl- β -cyclodextrin and doxorubicin pharmacokinetics and tissue concentrations following bolus injection of these drugs alone or together in the rabbit*". International Journal of Pharmaceutics, Volume 180, Issue 2, 15 April 1999, Pages 215-223.
- [14] Wayne L. Strauss, Matthew E. Layton and Stephen R. Dager, "*Characterization of human brain pharmacokinetics using a two-compartment model*". Biological Psychiatry, Volume 45, Issue 10, 15 May 1999, Pages 1384-1388.
- [15] Krishnaswami .S, Hochhaus .G, Mollmann .H, Barth .J and Derendorf .H, "*Interpretation of adsorption rate data for inhaled fluticasone propionate obtained in compartmental pharmacokinetic modeling*". International journal of clinical pharmacology and therapeutics, Volume 43, Issue 3, March 2005, Pages 117 -122.
- [16] J. Norman, "*The I.V administration of drugs*". British journal of Anaesthesia, Volume 55, Issue: 11 , 1983, Pages: 1049-1052.
- [17] Kwang Seok Kim and Laurent Simon, "*Optimal intravenous bolus-infusion drug-dosage regimen based on two-compartment pharmacokinetic models*". Computers & Chemical Engineering, Volume 33, Issue 6, 16 June 2009, Pages 1212-1219.
- [18] Mitenko and R.I. Ogilvie, "*Pharmacokinetics of intravenous theophylline*". Clinical Pharmacology and Therapeutics, Volume: 14, 1973, Pages: 509-513.
- [19] Norman W. Loney, "*Applied Mathematical methods for Chemical Engineers*". Second edition.
- [20] Richard Bronson, "*Schaum's easy outlines, Differential equations*". McGraw-Hill. 2003.